Science of the Total Environment 891 (2023) 164252

Contents lists available at ScienceDirect

Science of the Total Environment

journal homepage: www.elsevier.com/locate/scitotenv

Quantitative proteomic analyses of a Pb-adapted *Tetrahymena thermophila* strain reveal the cellular strategy to Pb(II) stress including lead biomineralization to chloropyromorphite

Patricia de Francisco [a], Francisco Amaro [a], Ana Martín-González [a], Aurelio Serrano [b], Juan-Carlos Gutiérrez [a,*]

[a] Department of Genetics, Physiology and Microbiology, Faculty of Biology, C/. José Antonio Nováis, 12, Complutense University of Madrid, 28040 Madrid, Spain
[b] Institute of Plant Biochemistry and Photosynthesis, CSIC-University of Seville, Av. Américo Vespucio 49, 41092 Seville, Spain

HIGHLIGHTS

- *T. thermophila* can perform Pb(II) biomineralization to chloropyromorphite (ClPm).
- Vesicular traffic promotes cellular ClPm bioaccumulation and its later expulsion.
- The stress response includes proteolysis, metallothioneins and antioxidant enzymes.
- The Pb-adapted strain can remove about 90 % of the toxic soluble lead from the medium.

GRAPHICAL ABSTRACT

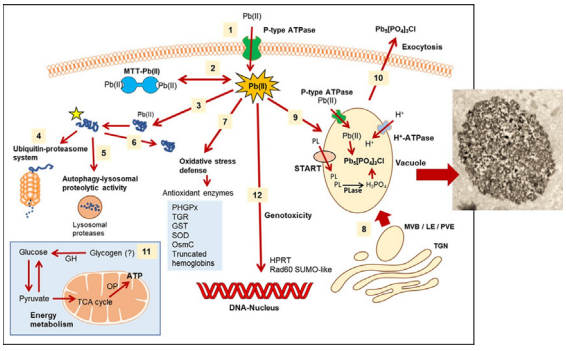

ARTICLE INFO

Editor: Julian Blasco

Keywords:
Chloropyromorphite
Proteomic
Oxidative stress
Metallothioneins
Vesicular traffic
Tetrahymena thermophila

ABSTRACT

A strain of the protozoan ciliate *Tetrahymena thermophila* adapted to increasing Pb(II) concentrations over two years has shown that one of the resistance mechanisms to this extreme metal stress is the lead biomineralization to chloropyromorphite, one of the most stable minerals in the earth's crust. Several techniques such as microanalysis coupled to transmission and scanning electron microscopy (X-Ray Energy Disperse Spectroscopy), fluorescence microscopy and X-ray power diffraction analysis have revealed the presence of chloropyromorphite as crystalline aggregates of nano-globular structure, together with the presence of other secondary lead minerals. This is the first time that the existence of this type of biomineralization in a ciliate protozoan is described. The Pb(II) bioremediation capacity of this strain has shown that it can remove >90 % of the toxic soluble lead from the medium. A quantitative proteomic analysis of this strain has revealed the main molecular-physiological elements involved in adaptation to Pb(II) stress: increased activity of proteolytic systems against lead proteotoxicity, occurrence of metallothioneins to immobilize Pb (II) ions, antioxidant enzymes to mitigate oxidative stress, and an intense vesicular trafficking presumably involved in the formation of vacuoles where pyromorphite accumulates and is subsequently excreted, together with an enhanced energy metabolism. As a conclusion, all these results have been compiled into an integrated model that could explain the eukaryotic cellular response to extreme lead stress.

1. Introduction

Lead (Pb) is a metal with a unique oxidation state (Pb^{2+}) that has no known biological function. It is considered one of the most toxic, and most abundant metals in our planet (Tchounwou et al., 2012). Due to

* Corresponding author.
E-mail address: juancar@bio.ucm.es (J.-C. Gutiérrez).

http://dx.doi.org/10.1016/j.scitotenv.2023.164252
Received 2 January 2023; Received in revised form 14 April 2023; Accepted 14 May 2023
Available online 26 May 2023

anthropogenic activity involving lead, such as the use of insecticides, industrial wastes, mining activity, gases released by cars, batteries, pigments, etc., it is considered one of the main environmental pollutants (Sharma and Dubey, 2005). In addition, being water-soluble, lead can be adsorbed by plant roots and thus incorporated into the food chain. Thus, it can reach humans via ingestion and/or inhalation, originating different types of pathologies that affect the nervous, cardiovascular, or respiratory system (Tchounwou et al., 2012).

Lead alters a large number of physiological processes due to the diversity of targets included in its toxicity mechanisms, of which the most relevant are: competition with essential metal cations such as calcium, disturbance of the transport of essential cations and the intracellular osmotic balance, disruption of protein biosynthesis and enzymatic activity by interacting with sulfhydryl and amide groups, generation of reactive oxygen species (ROS) leading to oxidative stress, lipid peroxidation, apoptosis, and DNA damage (Silbergeld et al., 2000; Jaishankar et al., 2014; Wu et al., 2016a, 2016b; Kumar and Prasad, 2018).

To resist the stress imposed by lead toxicity, prokaryotic and eukaryotic cells have developed several defense strategies and detoxification mechanisms, among which we can highlight the following: bioadsorption by extracellular polymers (Jarostawiecka and Piotrowska-Seget, 2014), efflux systems by P-type ATPases (Gillet et al., 2019), intracellular immobilization or sequestration by specific proteins (such as metallothioneins) (Gutiérrez et al., 2019) and oligopeptides (such as phytochelatins or glutathione) (Kumar and Prasad, 2018; Lee et al., 2019), and/or extra- or intracellular precipitation by biomineralization (Liang et al., 2016). These strategies are not exclusive, and several of them may appear concurrently in a single cell, depending on the degree of stress caused by lead.

Biomineralization has been defined as a process by which living beings stimulate the synthesis of minerals, which are immobilized by the cell and/or bioprecipitated (Rahman and Singh, 2020). Some authors have considered that this process can be classified into two categories (Gadd et al., 2012): a)- biologically induced mineralization, where an organism alters the environment by chemically modifying the toxic metal and excreting it as a precipitated insoluble mineral form generally as a detoxification mechanism (Jarostawiecka and Piotrowska-Seget, 2014), or b)- biologically controlled mineralization, where the organism has a high degree of control over the mineralization process, such as the complex external mineral structures formed by certain eukaryotic microorganisms, for instance; the tests or exoskeletal structures of diatoms, foraminifera or radiolarians (Dubicka and Gorzelak, 2017).

Lead can react with different anions such as chlorides, phosphates or hydroxyl radicals to form insoluble precipitates (induced biomineralization), and in this way different microorganisms decrease the concentration of free, bioavailable and toxic Pb(II) present in the medium (Naik and Dubey, 2013; Albi and Serrano, 2016). Pyromorphite (Pm) is a secondary lead ore that occurs abiotically in oxidized zones of lead deposits. Pm crystallizes in hexagonal prisms with a globular, reniform or granular morphology. There are several types of Pm: $Pb_5[PO_4]_3\times$, where "X" can be fluorine, chlorine, bromine, or a hydroxyl. Chloropyromorphite (ClPm) ($Pb_5[PO_4]_3Cl$) is the most stable Pb mineral in the earth's crust (Miretzky and Fernandez-Cirelli, 2008). The low solubility of this mineral reduces the Pb(II) bioavailability in contaminated soils, and the formation of this mineral has been proposed as a possible bioremediation mechanism (Clipson and Gleeson, 2012).

The biomineralization of lead to Pm as a Pb(II) detoxification mechanism has been described in both prokaryotes and eukaryotes. In the pathogenic Gram-negative bacterium *Burkholderia cepacia* the formation of hydroxypyromorphite (OHPm) nanocrystals was detected (Templeton et al., 2003). Among eukaryotes the transformation of Pb(II) to Pm has been described in several soil filamentous fungi (*Aspergillus niger* and *Paecilomyces javanicus*) (Rhee et al., 2012), in root-fungus symbiosis (mycorrhizae) (Bizo et al., 2017), yeasts (Liang et al., 2016; Sarkar et al., 2019) and in the nematode *Caenorhabditis elegans* (Jackson et al., 2005). The specific molecular mechanism to explain microbial lead biomineralization by releasing phosphate to form Pm is still little known, although some authors (Liang et al., 2016) have suggested the presence of exophosphatase activities that would increase the availability of inorganic phosphate in the extracellular medium, promoting the precipitation of Pm minerals on the cell surface (cell walls of bacteria or fungi) or outside the cell.

Stress-adapted organisms have not only been isolated from natural environments (Khan et al., 2015), but have also been generated in the laboratory under certain stress conditions which promote the development of new metabolic abilities or novel phenotypes (Sauer, 2001; De Francisco et al., 2018b). The progressive adaptation process to certain extreme conditions enhances the cellular resistance mechanisms to stress, becoming more evident and easier to be detected. The main purpose of this study was to analyze the physiological and cell structural features of a strain of *Tetrahymena thermophila* (ciliated protozoon) adapted over time to grow under increasing concentrations of Pb(II). Transmission electron microscopy (TEM), including TEM-microanalysis, and fluorescence microscopy of this Pb-adapted strain detected large Pb-rich cytoplasmic deposits, which were subsequently excreted out of the cell. The spectra obtained by TEM-XEDS (X-Ray Energy Dispersive Spectroscopy) of the intracellular deposits identified the lead mineral as ClPm. Furthermore, the scanning electron microscopy-XEDS (SEM-XEDS) revealed ClPm with an aggregated crystalline nano-globular structure. X-ray powder diffraction analysis (XRPD) confirmed the presence of ClPm, together with other secondary lead minerals, in the material excreted by the Pb-adapted cells. To our knowledge, this is the first time that a Pb(II) biomineralization process to ClPm is reported in a ciliated protozoon, and our results suggest that this Pb-adapted strain can detoxify Pb through cytoplasmic ClPm formation, discharge and extracellular deposition. To know more about this Pb(II)-adapted strain and the cell physiological changes on which this adaptation and the process of Pb(II)-biomineralization to ClPm are based, a quantitative proteomic analysis was carried out. From this analysis we infer that the main processes that stand out in the Pb-adapted strain are: a high activity of proteolytic systems (ubiquitin-proteasome and autophagy-lysosome) as a consequence of lead proteotoxicity, synthesis of metal-chelating metallothioneins and antioxidant enzymes to mitigate ROS formation, extensive vesicular traffic originating vacuoles where Pb(II) is biomineralized to ClPm and subsequently excreted to the medium, and a high energetic metabolism that supports the detoxification processes. From all these data, a model showing the cellular adaptive strategy to Pb(II) extreme stress and its biomineralization to ClPm is discussed.

2. Materials and methods

Due to the length of this manuscript, a detailed Materials and methods section has been included in supplementary material (see Text-1S).

3. Results

3.1. Isolation and characterization of a T. thermophila strain adapted to extreme lead concentrations

The adaptation process to Pb(II) consisted of gradually exposing *T. thermophila* (strain SB1969) to increasing concentrations of the metal over a two-year period, until the maximum tolerable concentration (MTC) was reached. The MTC value of the Pb-adapted strain was 5500 μM growing in PP210 medium, which is about 5.7 times the Pb LC_{50} of the control strain (965 μM) in this same growth medium. In Tris-HCl buffer the Pb LC_{50} value (800 μM) of the Pb-adapted strain is about 7.3 times higher than that of the wild type strain (110 μM). The analysis of the growth kinetic parameters from the Pb-adapted strain with respect to the control, showed that the growth rate and the generation time of the adapted strain are something different than the control culture and a moderate delay in cell growth of the Pb-adapted strain was detected (Table 1S).

3.2. Large and numerous electrodense deposits appear in the Pb-adapted strain

In both thin and ultrathin sections, a remarkable difference between control (Fig. 1A) and Pb-adapted cells (Fig.1B) is already apparent: the presence of large and numerous, spherical, or ellipsoidal, cytoplasmic inclusions or deposits containing an electrodense granular material surrounded by a membrane (Fig. 1C, D). The micrograph in Fig. 1D shows a cytoplasmic region with an intense network of vesicles or vesiculation (dashed line box), which might be the trans-Golgi network (TGN), and from where these vesicles containing the electrodense material could originate (Fig. 1D). Presumably, this granular material is accumulated inside vacuoles or secretion granules and ends up being expelled out of the cell, as compacted clusters of granular material that maintain the shape they acquired inside the vacuole or cytoplasmic container (Fig.1E). On average, more than ten clusters per cell, of different sizes and with a compacted granular content, have been detected (Fig.1F). To determine whether the presence of these deposits is a reversible process and depends on the presence of lead in the medium, the Pb-adapted strain (which is always kept under constant exposure to Pb) was maintained for one month without the presence of the metal, and then analyzed by TEM. Similarly, after one month without the metal, these cell populations were again exposed to the metal at MTC for 24 h, and again analyzed by TEM. As it is shown in Fig.2, a smaller number of remnant deposits with a lower content of electrodense particles (Fig.2A, 2B) are detected in cells maintained for one month without the metal, and no electrodense material excreted outside the cells is observed. When these cells are again exposed to Pb (24 h), deposits with condensed electrodense material, characteristic of Pb-adapted cells, appear again, and this material is expelled back out of the cell (Fig.2C, 2D).

Higher resolution TEM observations (TEM-XEDS-derived images) show that the electrodense granular material released from the cell consists of granules or nanoparticles of about 5–10 nm (Fig.3A), which have a crystalline structure (Fig.3B, 3C).

3.3. Detection of lead in the electrodense intracellular deposits by fluorescence and electron microscopy microanalysis

The use of Leadmium Green fluorochrome in the lead-adapted strain showed many green-fluorescing ovoid deposits (Fig.3E, 3F), which correspond to the refringent bodies detected in bright-field (Fig.3D). This highlights the presence of lead in these deposits, because this fluorochrome detects Pb or Cd. A more precise analysis of the elemental composition of these electrodense deposits was carried out by microanalysis using TEM-XEDS. The spectra obtained showed differences between the abiotic control (culture medium without the presence of the ciliate) and the Pb-adapted strain culture (Fig.4). In the cell-free control, lead and carbon were detected as the main elements (Fig. 4A), while the spectrum obtained directly from the electrodense intracellular deposits showed a pattern with Pb, P and Cl peaks (box in Fig. 4B) coincident with the phosphorus and chlorine containing lead mineral known as chloropyromorphite ($Pb_5[PO_4]_3Cl$). Likewise, the SEM-XEDS analysis of extracellular material (Fig. 5), excreted by the Pb-adapted strain (Fig. 5B) or from a control culture (without cells) (Fig. 5A), shown spectra like those from TEM-XEDS.

3.4. Identification of lead secondary minerals using X-ray powder diffraction analysis (XRPD)

Secondary Pb minerals were analyzed from extracellular material (excreted by cells) obtained from cultures with the Pb-adapted strain grown at MTC of lead, and an abiotic control (cell-free culture medium) exposed for one month to the same Pb concentration (5.5 mM). The XRPD analysis of the control sample showed a stick pattern or plot of identified phases corresponding to lead dioxide (PbO_2), present in a higher percentage (60 %) (Fig. 1SA), together with a minor component (40 %) of lead oxide carbonate hydrate, a type of hydrocerussite [$Pb_2(CO_3)O(H_2O)_2$] (Fig. 1SA). On the other hand, the sample of the material excreted by the Pb-adapted strain

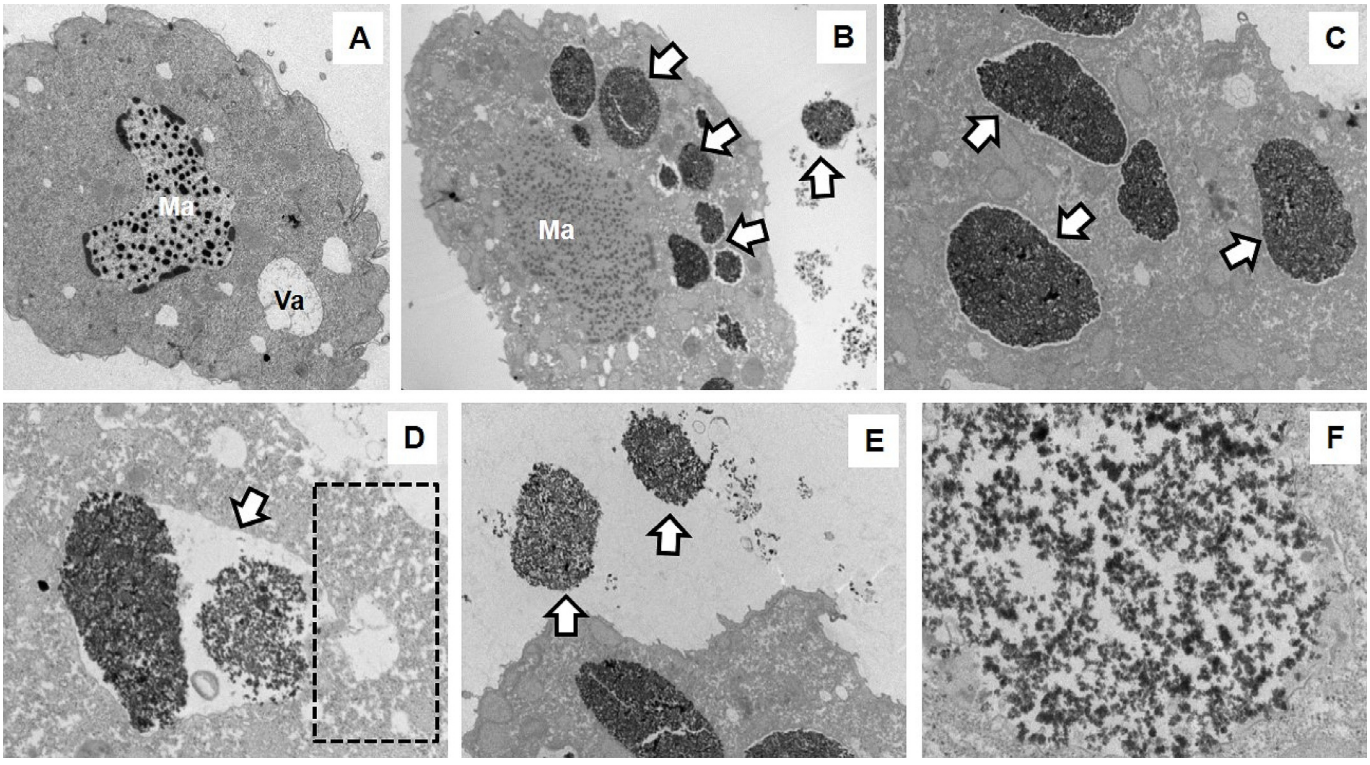

Fig. 1. Transmission electron microscopy (TEM) micrographs of control and Pb-adapted strains. (A)- control strain cell (6000 ×). (B—F)- Pb-adapted strain. (B)- electrodense inclusions inside vacuoles and outside the cell (white arrows) (6000 ×). (C)- enlarged image of electrodense material in vacuoles (arrows) (12,000 ×). (D)- electrodense granular-particulate material inside a vacuole (arrow indicates vacuolar membrane). The dashed line box shows an intense Golgi vesicular network (25,000 ×). (*E*)- electrodense material ejected from the cell (arrows) (12,000 ×). (F)- enlarged image of the electrodense granular-particulate material (50,000 ×). Ma: macronucleus, Va: vacuole.

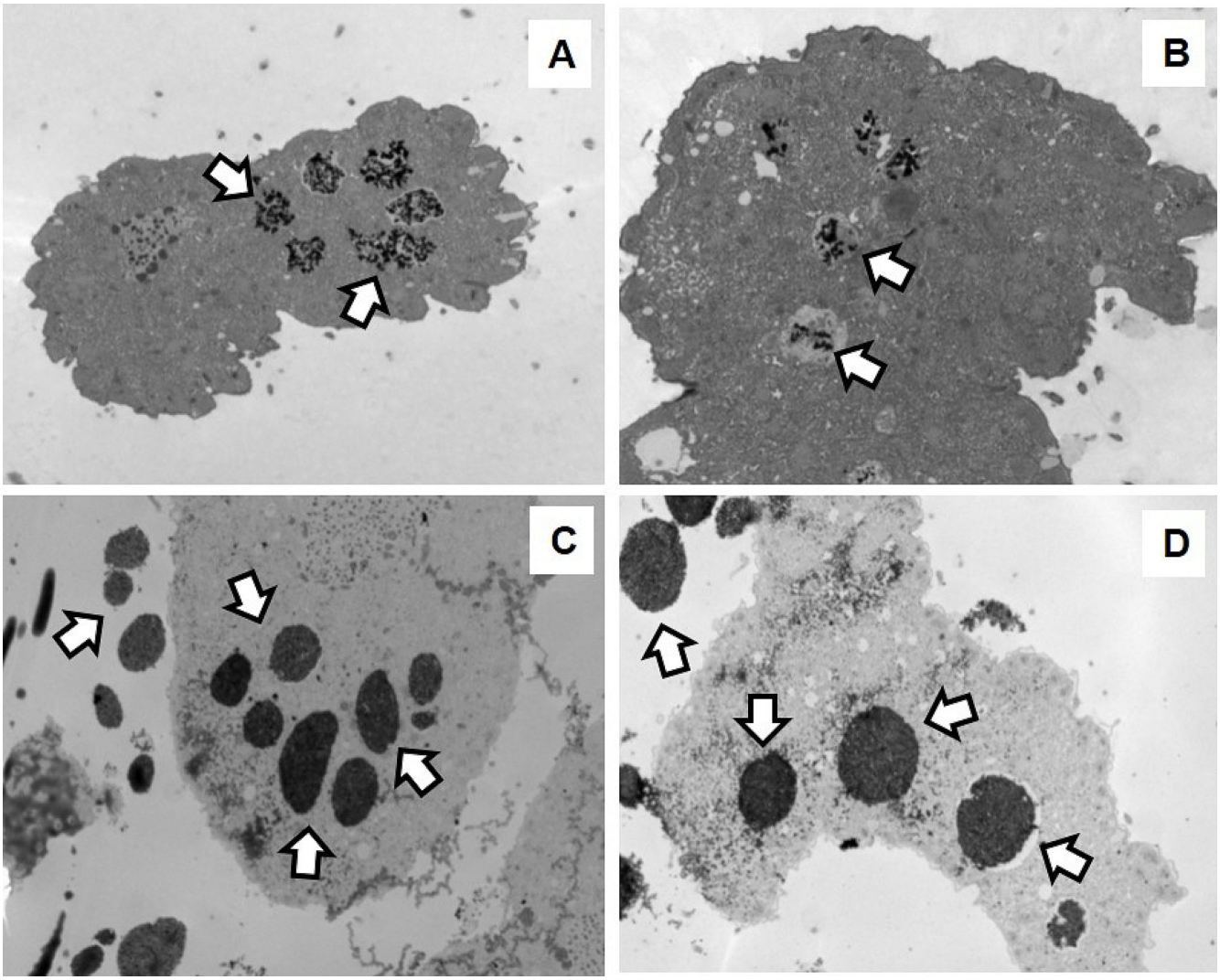

Fig. 2. TEM micrographs of Pb-adapted strain. (A) and (B)- Pb-adapted cells after one month without Pb exposure. Vacuoles with a residual content of electrodense particles (arrows) (5000× and 8000×, respectively). (C) and (D)- Pb-adapted cells after one month without Pb exposure and re-exposed to Pb (5.5 mM) for 24 h. Electrodense material in vacuoles and outside the cell (4000× and 5000×, respectively).

showed a plot of identified phases corresponding to chloropyromorphite ($Pb_5[PO_4]_3Cl$) (Fig. 1SB). In addition, lead oxide (PbO) has also been detected in some samples from Pb-adapted strain (Fig. 1SC).

3.5. Analysis of the bioremediation capacity of the Pb-adapted strain

Using induced coupled plasma optical emission spectrometry (ICP-OES) technique, the amount of lead removed from the medium by the Pb-adapted strain was calculated after maintaining the Pb-adapted cells in it for 24 or 48 h, at two different Pb concentrations (200 or 500 μM or their equivalent concentrations measured by ICP-OES: 45 or 120 μg/ml). As shown in Fig. 6A, the Pb-adapted strain can remove >90 % of the Pb^{2+} present in the medium in only 24 h, regardless of the initial starting concentration. After 48 h of incubation, a slight increase (2.5 %) in the remaining amount of Pb present in the medium was detected, only in the assay performed at a higher Pb concentration (Fig. 6A), which could be due to some mortality of the cell population after 48 h of exposure.

To elucidate the toxicity degree of the medium after removal most of the metal by the Pb-adapted strain, a series of bioassays were carried out with a control strain (SB1969) of this ciliate. This control strain was exposed to both, the supernatant of a culture from the Pb-adapted strain grown for 5 days in PP210 medium with lead (5.5 mM, initial concentration), or the insoluble (precipitate material) excreted by the Pb-adapted strain during its growth. Mortality percentages were measured by flow cytometry, and several control cultures were used: a control culture exposed to 800 μM Pb concentration (which is the Pb(II) LC_{50} value for the Pb-adapted strain in Tris-HCl), a standard culture (live control) without Pb and a culture with dead cells after fixation with 37 % formaldehyde (Fig. 6B). The control strain (SB1969) shows high mortality (~87 %) when exposed to the Pb concentration corresponding to the LC_{50} for the Pb-adapted strain. In contrast, the percentage of mortality obtained from exposure to the supernatant from the Pb-adapted strain culture (previously grown for 5 days) is very low (1.35 %), and thus reducing mortality by ~85 %. However, the control culture exposed to the material excreted by the Pb-adapted strain showed some mortality (~21 %) (Fig. 6B), and in this case the reduction in mortality was only ~65.5 %.

3.6. Relative quantification and comparative proteomic analysis

For a better understanding of the adaptive cellular response to high concentrations of Pb, and its biomineralization to chloropyromorphite, a quantitative proteomic analysis of the Pb-adapted *T. thermophila* strain was carried out by LC/MS with respect to a control strain (SB1969). A total of 1790 proteins were identified as *T. thermophila*-derived proteins, of which 949 (~53 %) from the control sample and 841 (~47 %) from the Pb-adapted strain. Uncharacterized or hypothetical proteins were detected in

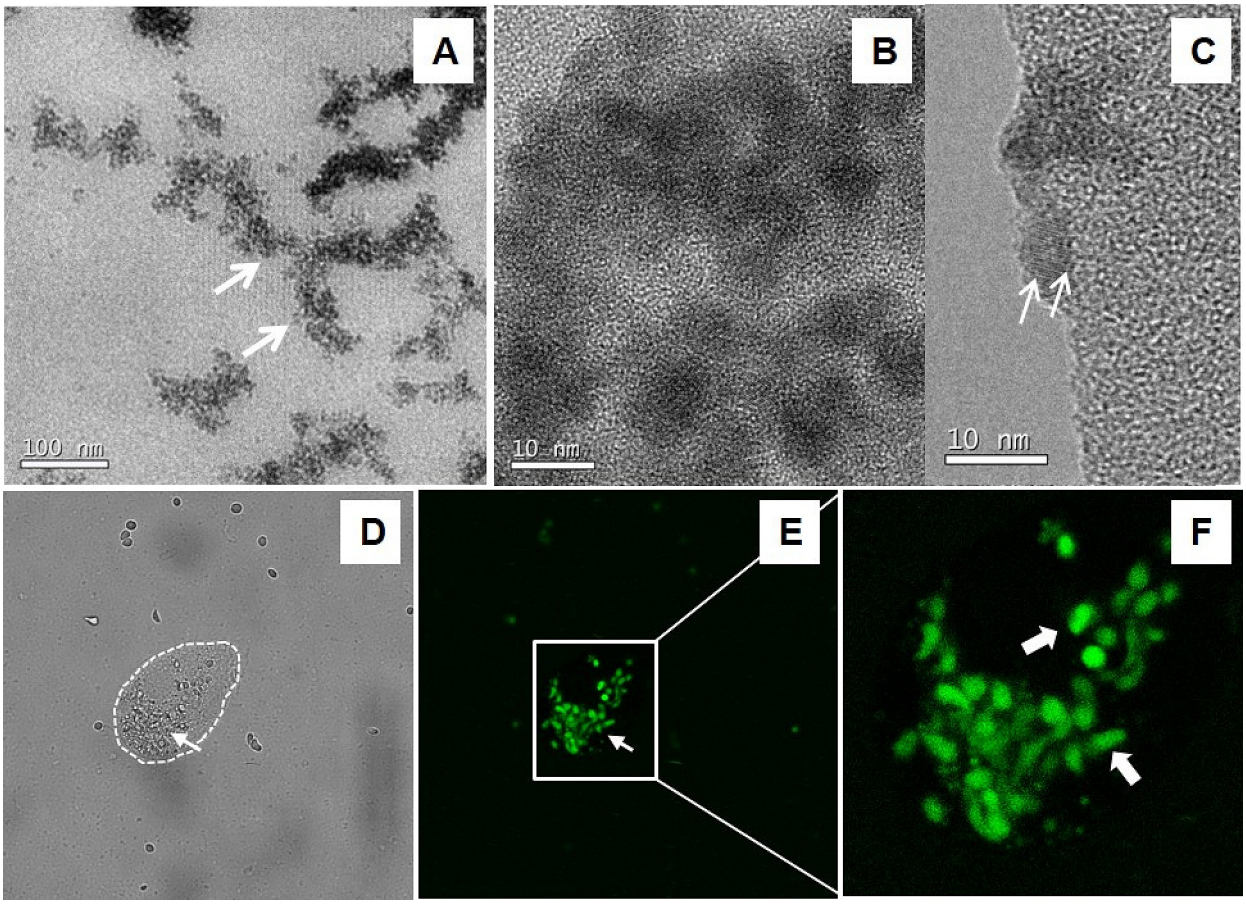

Fig. 3. (A-C)- High resolution images derived from microanalysis (TEM-XEDS), showing the crystalline structure of nanoparticles corresponding to the particulate electrodense material detected inside vacuoles in the Pb-adapted strain. (D—F)- Confocal fluorescence microscopy micrographs of the Pb-adapted strain. (C)- shows the crystal structure (arrows) of a nanoparticle. (D)- Brightfield image of a cell (outline is indicated by dashed line), arrow indicates refringent content (600×). (E)- staining of the refringent content with Leadmium Green fluorochrome of the same cell shown in (D) (600×). (F)- magnified image of the same cell (1000×). Arrows indicate ellipsoidal deposits containing Pb, which would correspond to the electrodense vacuolar content detected by TEM (Fig. 1).

both samples; 107 (11.27 %) from the control strain and 85 (10.10 %) from the Pb-adapted strain. This represents a 10.72 % of the total number of proteins (1790) detected between both strains.

From the 841 Pb-adapted strain characterized proteins, those (266 proteins) with a relative fold increase value ≥1.49 with respect to the control strain were selected and classified into different functional groups (Table 2S). The different functional groups and the percentage of proteins included in each of them for the Pb-adapted strain are shown in Fig. 7. The two major functional groups are proteins involved in proteolysis processes (11.27 %) and reducing the oxidative stress (11.27 %) caused by Pb. The next two largest groups are proteins involved in vesicle formation or membrane trafficking (9.39 %) and energetic metabolism (8.27 %) (Fig. 7). Transmembrane and/or transport proteins comprise 7.14 %. The groups related to oxidative phosphorylation and ubiquitin-proteasome system represent about 6.0 % each, and stress proteins group account for 6.39 %. A significant group of proteins related to metal stress are metallothioneins (metal- chelation), and this group represents only 1.12 % of the total amount of proteins characterized in the Pb-adapted strain, however it includes the two proteins (metallothioneins MTT5 and MTT1) that reached the highest increases in this strain (51.14- and 30.90-fold, respectively, compared to the control strain).

The picture of the functional groups from the control strain is very different (Table 3S, Fig. 8). Most increased proteins identified in log-phase *T. thermophila* cells, regarding the Pb-adapted strain, are related to the translational machinery (22.49 %), followed by some proteins associated with DNA or ciliate macronucleus (13.98 %). Like in the Pb-adapted strain, in the control strain the proteins included in the transmembrane transport functional group are significantly numerous (9.72 %) (Fig. 8).

There are functional groups that appear in both strains, but their proportional amount is very different between them, for example, cytoskeleton (5.16 %-control vs 2.25 %-Pb-adapted), translation machinery (22.49 %-control vs 4.51 %-Pb-adapted), signaling (3.34 %-control vs 1.50 %-Pb-adapted), oxidative stress (1.82 %-control vs 11.27 %-Pb-adapted), proteolysis (1.21 %-control vs 11.27 %. Pb-adapted) and so on (Figs. 7 and 8).

The top ten most abundant proteins in one strain relative to the other and vice versa are shown in Fig. 9. The functional groups in which the 10 most abundant proteins of both strains have been included do not coincide. In the Pb-adapted strain most of these proteins are included in three main groups, namely metal chelation, oxidative stress, and proteolysis, whereas half of the ten most abundant proteins in the control strain are included in the functional group related to DNA and macronucleus.

As the macronuclear genome of *T. thermophila* is polygenic, consisting of gene families including several paralogs, both the control and Pb-adapted strains overexpress paralog genes encoding isoforms of the same type of enzyme (isoenzymes) or protein. Each of these gene versions is differentially expressed quantitatively and qualitatively in both strains. Figs. 2S to 4S show some examples of different protein isoforms that are identified as members of the same set of enzymes, proteins with similar structural domains or of the same family within the same functional group. Each strain expresses mostly and selectively one or several isoforms, for example, from the 62 isoforms of glutathione-S-transferase (GST) found in the

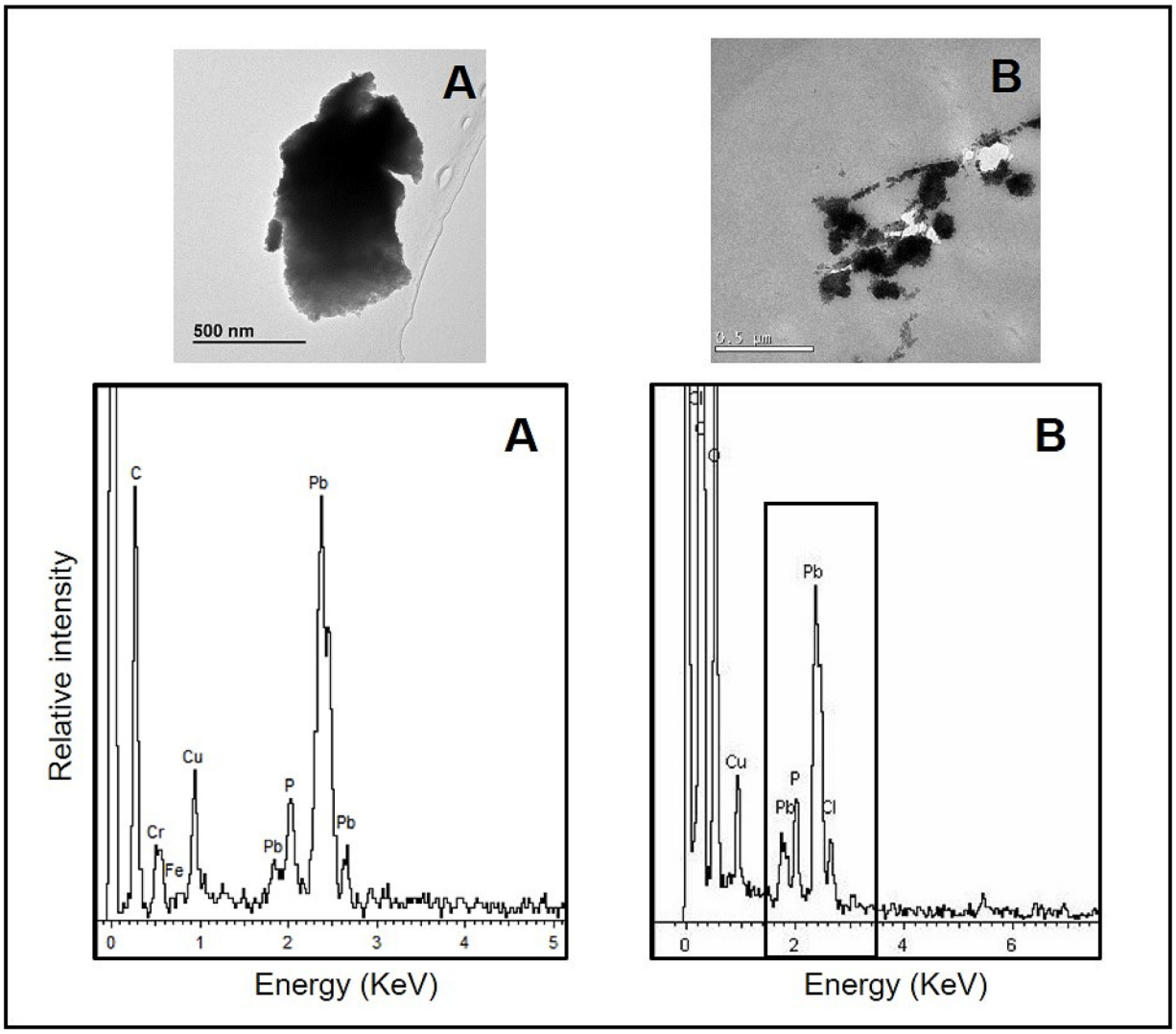

Fig. 4. Spectra obtained by TEM-XEDS analysis. (A)- abiotic control (no cells). (B)- sample from the Pb-adapted strain. TEM micrographs show fragments of the samples on which elemental microanalysis was performed.

T. thermophila genome (included in oxidative stress functional group), 5 of them appear predominantly in the Pb-adapted strain, with respect to the control strain, whereas 3 isoforms, different from the previous ones, appear in the control at higher levels than in the Pb-adapted strain (Fig. 2S). In other functional groups (Fig. 3S) such as proteolysis, 7 isoforms of cysteine proteases from the papain family are detected in the Pb-adapted strain, and none in the control. On the other hand, in the transmembrane and/or transport protein group, only one ABC family transporter protein appears in the Pb-adapted strain, while in the control there are four different proteins from this functional family (Fig. 4S).

4. Discussion

4.1. Adaptation of T. thermophila cells to elevated lead concentrations

In controlled-evolution experiments, the aim is to obtain organisms with certain physiological capacities in a relatively rapid and controlled manner. For this purpose, organisms are subjected to certain stress conditions (presence of drugs, extreme temperature, salinity, etc.), which are increased gradually and continuously over time to obtain in a selective way adapted strains capable of surviving in these extreme conditions. The adapted organisms enhance all the defense mechanisms necessary to counteract this critical situation, thus facilitating their study. In general, these adaptive processes involve changes in the genome of organisms at various levels: changes in the expression levels of certain genes, the appearance of point mutations or intragenomic reorganization processes (De Francisco et al., 2018b). All these changes give rise to new phenotypes, adapted against a certain type of stress (Huang and Agrawal, 2016).

After the Pb(II) adaptation process in the ciliate *T. thermophila*, a maximum tolerable concentration (MTC) value of about 5.7 times the Pb LC_{50} value was reached in growth medium and about 7.3 times in Tris-HCl buffer. Unlike what occurs in strains of this ciliate adapted to high concentrations of Cd or Cu, in which there is an increase of 9 or 8 h in the generation time (Tg) with respect to the control (data not shown), in the Pb-adapted strain it is only about 1 h. Therefore, we consider that there is only a moderate delay in the growth of the Pb-adapted strain. However, there is a slight decrease in the cell density achieved with respect to the control culture. This means that over time the selection process applied (lead concentration increasing) has selected certain cells that grow optimally under these extreme conditions. Thus, the defense mechanisms involved in the neutralization of Pb(II) toxicity must be very efficient to keep their division rate almost intact. As in *Tetrahymena* Pb-adapted strain, the Pb-treated yeast *Papiliotrema laurentii* (Sarkar et al., 2019) showed similar growth parameters with respect to the control culture, although the cell density achieved was clearly lower.

Using electron microscopy (TEM) analyses, large and electrodense deposits have been detected inside vacuoles or secretion vesicles with a granular content. The content of these vacuoles or vesicles is expelled out of the

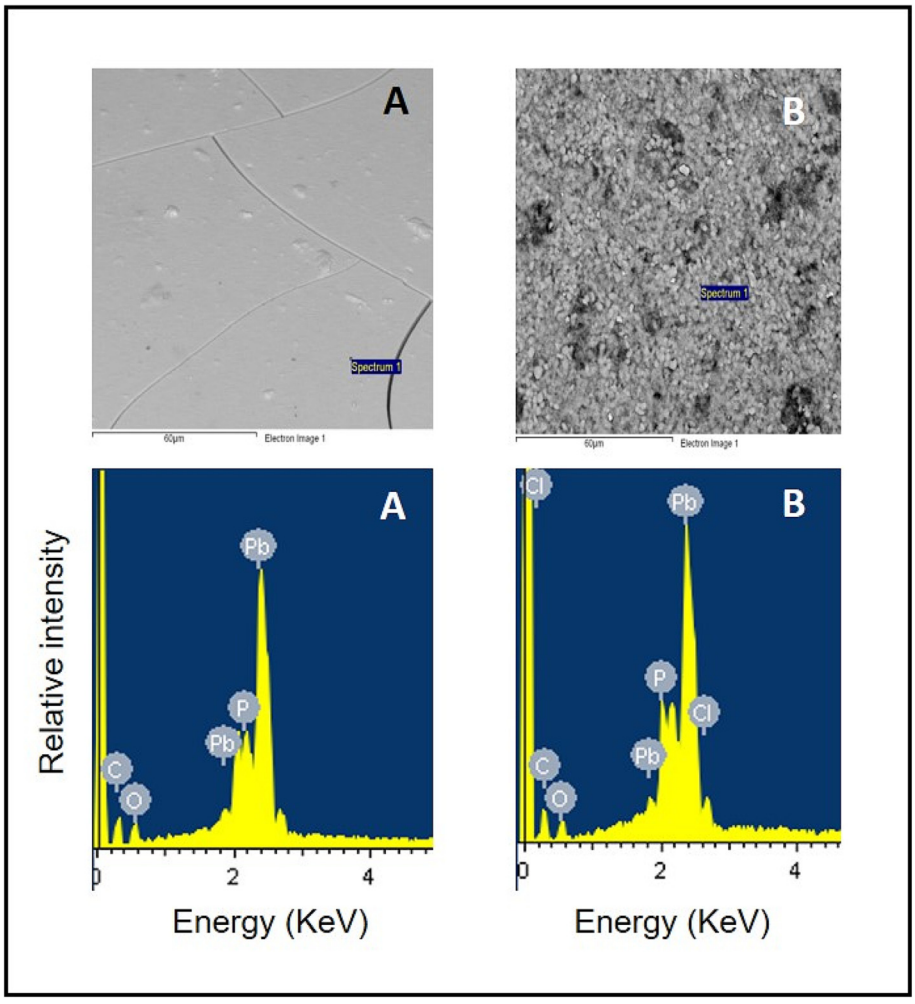

Fig. 5. Spectra obtained by SEM-XEDS analysis. (A)- abiotic control (no cells). (B)- sample of the material excreted by the Pb-adapted strain. The SEM micrographs show the regions or areas (marked as Spectrum 1) of the samples on which the elemental microanalysis was performed. The sample with material excreted by the cells (micrograph B) shows a granular or particulate appearance, in contrast to the smooth surface from the control.

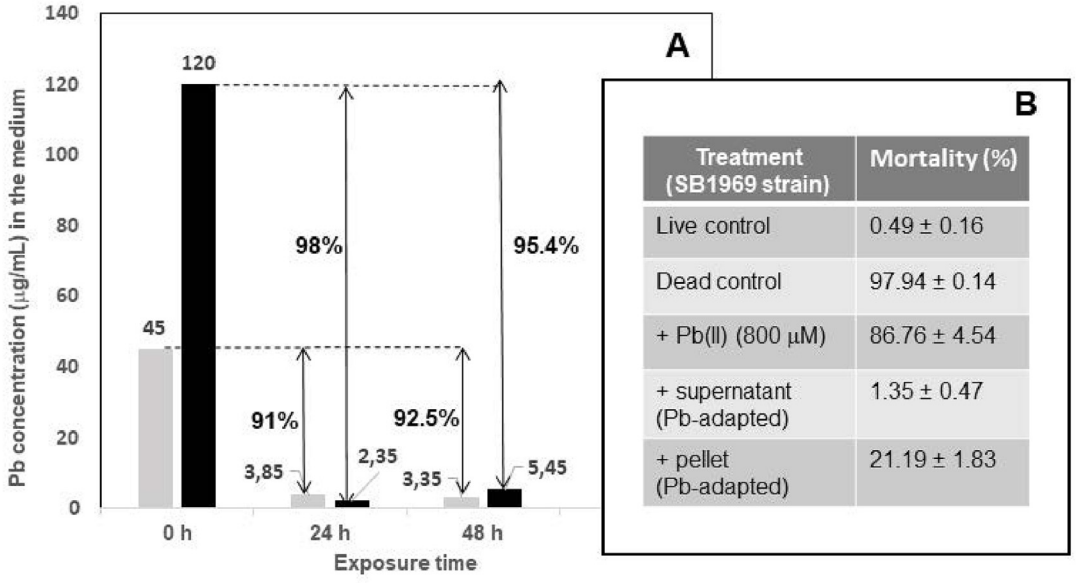

Treatment (SB1969 strain)	Mortality (%)
Live control	0.49 ± 0.16
Dead control	97.94 ± 0.14
+ Pb(II) (800 µM)	86.76 ± 4.54
+ supernatant (Pb-adapted)	1.35 ± 0.47
+ pellet (Pb-adapted)	21.19 ± 1.83

Fig. 6. Lead bioremediation capacity by the Pb-adapted strain. (A)- Histogram of Pb(II) concentrations in the medium before and after exposure to the Pb-adapted strain. Two different initial concentrations were used (200 and 500 µM). (B)- Mortality percentages measured by flow cytometry of the control strain under different conditions. For further explanation, see text.

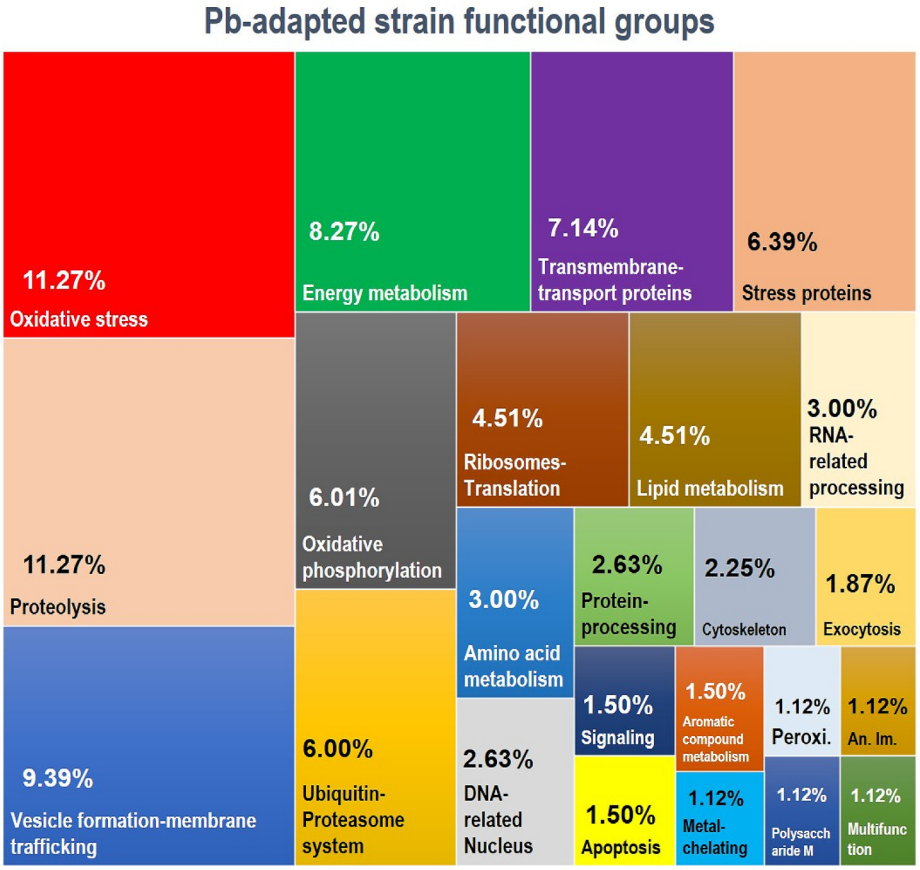

Fig. 7. Protein functional groups found in the Pb-adapted strain. The abundance (%) of proteins included in each functional group are indicated. See Table 2S for the proteins included. Peroxi (Peroxidation), Am. Im. (Antigenic immobilization - Immune system), Polysaccharide M. (Polysaccharide metabolism).

cell, after fusion of the vacuole or vesicle membrane with the ciliate envelope, releasing a compact granular content that maintains the ellipsoidal or spherical shape of the vacuole that contained it. These intra-vacuolar electrodense deposits are caused by the presence of lead at high concentrations, since when the metal is removed from the medium for a month, the cells only maintain small residual deposits of this granular material and stop expelling its content to the medium, and when again they are exposed for 24 h to the same Pb(II) concentration they return accumulate this material in vacuoles and expel it outside the cell.

The ability of *Tetrahymena* to bioaccumulate lead was reported by J.R. Nilsson in 1989 (Nilsson, 1989), who described the presence of dense granules in the cytoplasm and inside some organelles (such as mitochondria) when the ciliate was exposed to a lead sub-lethal concentration. Likewise, some marine protozoa have a great capacity to bioaccumulate lead in digestive vacuoles, thus reducing the presence of lead in the environment (Fernández-Leborans et al., 1998). Cyanobacteria (Burgos et al., 2013) accumulate lead as cytoplasmic inclusions composed of polyphosphates. The presence of lead in the electrodense granular material present in vacuoles of the Pb-adapted *Tetrahymena* strain was confirmed by fluorescence microscopy using Leadmium Green fluorophore.

4.2. Presence of chloropyromorphite in electrodense vacuolar or vesicular deposits

Both TEM- and SEM-XEDS microanalysis spectra of the electrodense granular vacuolar material and that expelled by the Pb-adapted strain showed the presence of the mineral known as chloropyromorphite, one of the most stable lead minerals. By high resolution TEM it could be observed that the vacuolar granular material was formed by nanoparticles (5–10 nm) of crystalline structure, which would correspond to this type of lead mineral. *T. thermophila* is capable of extracellularly producing silver nanoparticles from $AgNO_3$ after reduction of silver ions, which is also a cellular mechanism of stress response to this toxic metal (Juganson et al., 2013).

The biomineralization of lead to pyromorphite and other secondary minerals has been described in both prokaryotic and eukaryotic microorganisms that usually live in edaphic ecosystems. In biofilms formed by the bacterium *Burkholderia cepacia*, the presence of hydroxy-pyromorphite (OHPm) nano-crystals has been described, and their presence is due to the capacity of this bacterium to biomineralize intracellularly bioaccumulated Pb(II) (Templeton et al., 2003). Likewise, pyromorphite crystals have been detected in bacterial biofilms isolated from lead pipes (Menor-Salvan, 2012). Among eukaryotes, biomineralization of lead to pyromorphite has been described in both filamentous fungi and yeasts. For example, inside the hyphae of *Paecilomyces javanicus* (Rhee et al., 2012, 2014), in the yeast *Papiliotrema laurentii* which bioprecipitates lead in the form of phosphate and chloropyromorphite (Sarkar et al., 2019), and in root-fungus symbiosis (mycorrhizae) (Bizo et al., 2017). Also, the biological formation of OHPm crystals has been described in the nematode *Caenorhabditis elegans*, which bioaccumulates them in the anterior pharyngeal region after ingestion of lead nitrate (Jackson et al., 2005).

A secondary lead mineral as lead oxide (PbO) or litharge was detected, after using XRPD analysis, in the material presumably excreted by *Tetrahymena* cells. On the contrary, the abiotic control sample (without *Tetrahymena* cells) showed the presence of lead dioxide (PbO_2) in a high percentage together with a type of hydrocerussite (lead oxide carbonate hydrate). In a similar way, in samples of treated cultures of the fungus *P. javanicus*, both hydrocerussite [$Pb_3(CO_3)_2(OH)_2$] and PbO were detected, in addition to ClPm, while Pb and litharge (PbO) were detected in the control sample (Rhee et al., 2014). From these data we can infer that the presence or absence of a microorganism in the medium induces the formation of different secondary lead minerals.

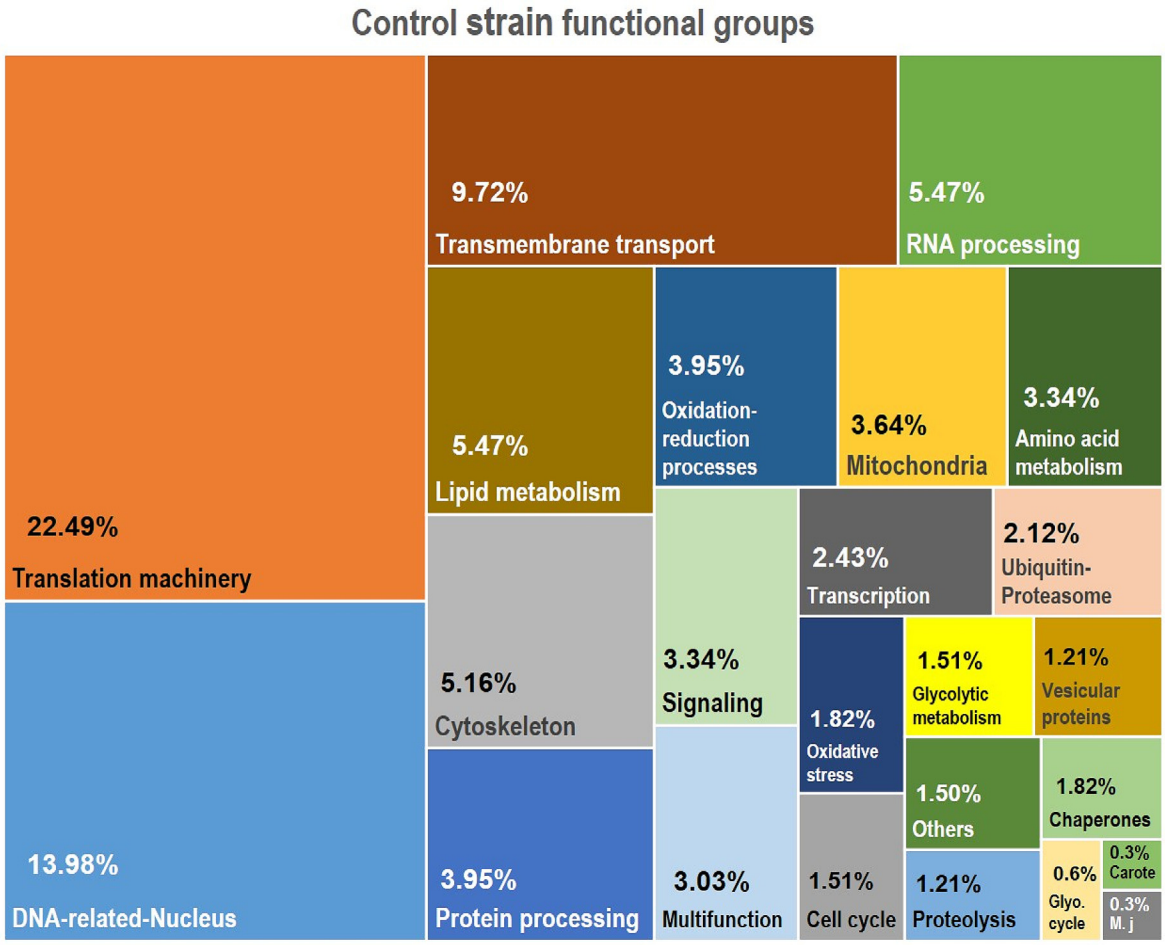

Fig. 8. Protein functional groups found in the control strain. The abundance (%) of proteins included in each functional group are indicated. See Table 3S for the proteins included. Glyo. cycle (Glyoxylate cycle), Carote. (Carotenoids), M.j. (Membrane junctions), The term "Other" includes Sulfur metabolism. Penicillin biosynthesis, N-Glycan biosynthesis, and Carbohydrate metabolism.

4.3. Bioremediation capacity of the lead-adapted strain

In metal bioremediation, both biomineralization and bioprecipitation, together with biosorption, have been used since these processes immobilize the metal making it non-bioavailable and thus decreasing its potential toxicity for living beings (Liang et al., 2016; Rahman and Singh, 2020). Bioremediation is based on the use of macroorganisms (plants), microorganisms (bacteria, fungi, or microalgae) or metabolic products originating from them to eliminate or block toxic pollutants (organic or inorganic) (Wang and Chen, 2006; Kuroda and Ueda, 2010). Strains resistant or adapted to metals are good candidates for bioremediation of ecosystems contaminated with these inorganic toxicants (Malik, 2004). These strains can be isolated from contaminated natural environments (Wu et al., 2016a, 2016b) or obtained in the laboratory (Geva et al., 2016), either by improving their resistance capacity by genetic engineering or by evolutionary adaptation experiments without the need to introduce foreign genes into the organism. This last possibility is less conflicting with international regulations when organisms need to be applied directly (in situ) in the contaminated environment.

Overall, our experiments carried out with the Pb-adapted and control strain show that the Pb-adapted strain can remove about 90 % of the lead present in the medium within 24 h. In the yeast *P. laurentii*, which bioprecipitates lead in the form of phosphate and chloropyromorphite, it was determined that it removes about 77.7 % of lead from the medium (Sarkar et al., 2019). The gram-positive bacterium *Bacillus subtilis* has a high ability to biomineralize lead by forming OHPm, and its ability to remove Pb(II) was estimated to be 381.3 mg/g of bacterial biomass in aqueous solution. The bacterium L. *adecarboxylata*, can immobilize lead by originating both OHPm and ClPm (Jiang et al., 2020).

So, the eukaryotic microbial strains adapted to high concentrations of lead, like the one described in this work, can be useful biotechnological tools in the bioremediation of this metal in polluted soil or aquatic habitats. Environmental contamination by metals is usually multiple (containing more than one toxic metal), so a bioremediation process must also consider the possibility of removing more than one type of metal from a polluted ecosystem.

An additional advantage of these metal-adapted microorganisms is that they can often exhibit cross-resistance phenomena to other metals or other types of environmental stressors (like antibiotics) (Baker-Austin et al., 2006). The *Tetrahymena* Pb-adapted strain is able to grow (with growth parameters similar to the control strain) under 4 mM Cu(II) ($CuSO_4$), that is the MTC value in a Cu-adapted strain from this ciliate, which is about 12 fold the LC_{50} value of the wild-type strain (data not shown), thus showing a cross-resistance to high concentrations of Cu(II). Furthermore, treatments of the Pb-adapted strain with toxic-metal mixtures (5.5 mM Pb(II) *plus* 2 mM Cu(II) or 57.5 μM Cd(II), these last two concentrations represent half of the MCT values for two other Cu- or Cd-adapted strains from this ciliate) have shown that it does not resist an exposure to the mixture (Pb + Cu), whereas it can grow under the mixture (Pb + Cd), although with a generation time about 3-fold longer than the control strain (data not shown).

Previous works using *T. thermophila* and other ciliates (Díaz et al., 2006; Gallego et al., 2007) have shown that mixtures of metals (such as Cd and Zn) can increase the intracellular bioaccumulation levels of both metals

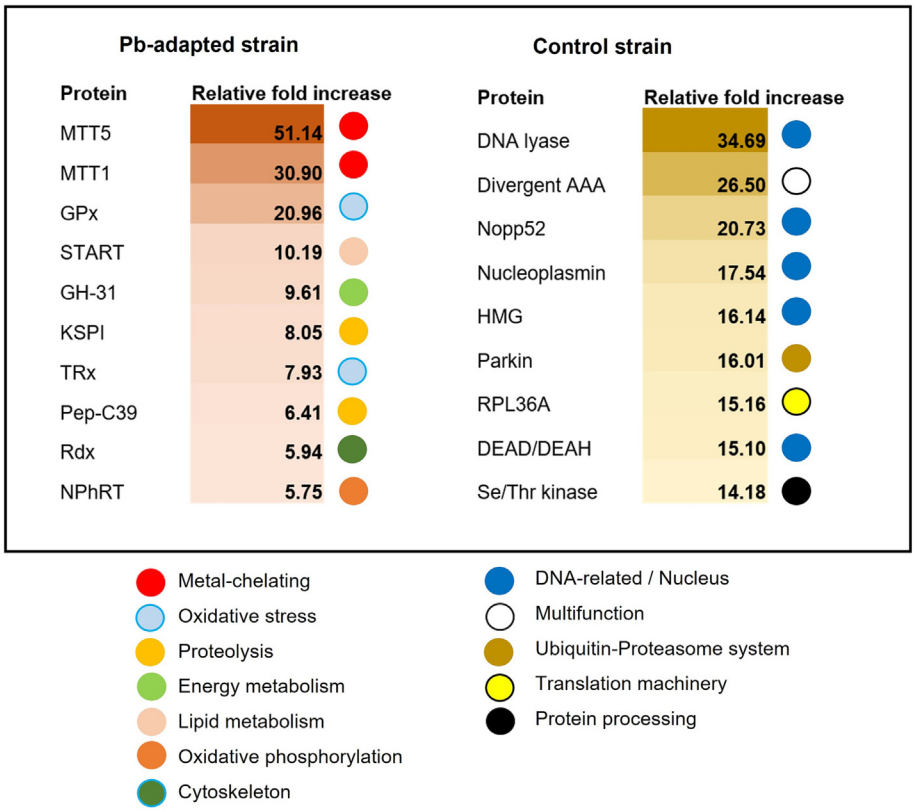

Fig. 9. The top ten most abundant proteins included in functional groups in each of the two strains analyzed (control and Pb-adapted). See Tables 2S and 3S for the identification of each of them and the functional groups.

after increasing their concentrations in the medium, mainly in soil ciliates that are more resistant to Cd (Díaz et al., 2006). Likewise, it has been shown that in some ciliates the presence of moderate Zn concentrations increases the intracellular bioaccumulation of Cd (Dunlop and Chapman, 1981; Martin-González et al., 2006). All these studies support the possibility of using microorganisms for multiple metal bioremediation in a contaminated ecosystem.

4.4. Quantitative proteomic analysis: towards a global view of the cellular stress response and adaptation to lead toxicity

Clustering of the characterized proteins into functional groups has revealed major differences between the two *T. thermophila* strains; the Pb-adapted and the wild type. Paralog genes present in the *T. thermophila* genome encode different protein versions or isoforms (Eisen et al., 2006). These genes can be differentially expressed in both strains (Pb-adapted and control) or in only one of them, acting as ecoparalogs whose expression depends on environmental conditions (Syutkin et al., 2014). The comparative analysis of these functional groups and the amount of different protein isoforms they contain will give us an idea of the cellular scenario existing in the Pb-adapted strain with respect to the control.

The increase of a certain protein in the Pb-adapted strain, with respect to the control, can be interpreted in two different ways; a)- that this protein is blocked or altered by Pb or it displaces the essential metal of the enzyme making it non-functional, and for that reason it is required to increase its production, or b)- that this protein is involved in the mechanisms of cellular resistance to Pb and thus requires to increase its presence in the stressed cells.

4.5. Proteolysis and ubiquitin-proteasome system

Lead interacts with the sulfhydryl groups of proteins, forming a flexible bond with oxygen and sulfur to form stable complexes that increase the affinity of Pb for the protein. In addition, the free radicals originating from Pb interact with polypeptides, through a metal-catalyzed oxidation of the protein. The interaction between the protein and the free radicals causes modifications in certain amino acids, which increases the vulnerability of the protein to proteolysis (Lee et al., 2019; Kumar and Prasad, 2018). The cellular stress response to Pb proteotoxicity is revealed by elevated levels of proteolysis. Protein degradation is accomplished by two ways; the autophagy-lysosomal proteolytic activity and the ubiquitin-proteasome system. Both play an important role in the stress response by removing damaged proteins, preventing their accumulation in toxic aggregates, and eliminating proteins with altered functions (Flick and Kaiser, 2012). In addition, proteolysis-regulated destruction of regulatory molecules constitutes a pathway for cell growth control (Tansey, 1999).

In the Pb-adapted strain, the largest functional group of increased proteins is composed of enzymes involved in proteolytic processes; a total of 30 (11.27 %) identified compared to the 4 that appear increased in the control strain with respect to the Pb-adapted strain. This group (proteolysis) is not only the most numerous, but also includes two of the 10 most abundant proteins of the Pb-adapted strain, namely KSPI (Kazal-type serine proteinase inhibitor) and Pep-C39 (peptidase C39 family), about 8- and 6-fold more abundant respectively with respect to the control. In the macronuclear genome of *T. thermophila* there are 23 gene isoforms for the KPI (Kazal-type proteinase inhibitor), of which only one is significantly increased in the Pb-adapted strain with respect to the control one. The second most abundant protein in the Pb-adapted strain is a C39 peptidase, of which there are only two homologs in the genome of *T. thermophila*. This cysteine peptidase is found in a wide range of ABC transporters. The protein or polypeptide they transport is processed (removal of the peptide leader) by the endopeptidase activity located in the N-terminal domain of the ABC transporter. In the Pb-adapted strain there are numerous transmembrane transporter proteins, so it could be thought that some of them could use this domain for the processing and transport of certain proteins.

About 480 protease-encoding macronuclear genes have been recorded in *T. thermophila* (Eisen et al., 2006), constituting 1.7 % of the total genomic pool, which is close to the 2 % found in many organisms (Rawlings et al., 2004). The Pb-adapted strain presents 30 proteases in a 1.49-fold higher level compared to the control, which means 6.25 % of the total number of protease genes from *T. thermophila*. From these, the largest group of isoforms present in the Pb-adapted strain is the papain family cysteine proteases (7 isoforms). This family has 225 homologs (46.8 % of the total number of protease genes), of which 7 (3 %) are present in the Pb-adapted strain, whereas none of them appear in the control in a significant amount. Five of them are identified as cathepsins (Fig. 3S), which are a group of lysosomal proteases, whose main function is protein recycling within lysosomes. A transcriptomic analysis of the *T. thermophila* stress response to silver nanoparticles (Piersanti et al., 2021) has shown overexpression of the cathepsin CTH7 and down-regulation of CTH12. CTH7 does not appear among those detected in the Pb-adapted strain (Fig. 3S), indicating that the proteolytic processes associated with these stress responses may be different.

The next most numerous proteinase isoform group identified in the Pb-adapted strain is the Peptidase M16 family, with 4 representatives and none in the control strain (Fig. 3S), from 23 isoforms present in the *T. thermophila* genome. This family also includes insulysins or insulinases, cytoplasmic enzymes involved in the processing of insulin, glucagon, and other small hormonal peptides. In many multicellular organism cells, the formation of autophagolysosomes is accelerated by the deficiency of insulin, essential amino acids, or glucagon (as in liver cells) (Lecker et al., 2006). The Pb-adapted strain overexpresses two insulysin isoforms while only one in the control, from seven different isoforms in the genome of this ciliate. They belong to a family of metalloproteases, which require divalent cations (usually zinc) for their activity. About 139 enzymes within this protease category have been identified in the genome of *T. thermophila*. Many of these enzymes contain the HEXXH motif (where "X" is any amino acid), which is part of the metal binding site. From the seven (between both strains) reported to appear in an amount >1.49-fold with respect to each strain (Fig. 3S), only one of them, identified as insulysin (TTHERM_01108740) has the above motif. Finally, of the 14 homologs for peptidase M1 in the genome of this ciliate, only one appears in similar and significant amounts in each of the strains (Fig. 3S). This type of aminopeptidases also belongs to the metalloproteases and are characterized by two motifs in the catalytic domain; a zinc-binding motif HEXXH-(X_{18})-E and an exopeptidase motif GXMEN (where "X" is any amino acid) (Albiston et al., 2004). The M1 peptidase isoforms identified in the compared strains (Pb-adapted and control) have both domains.

The 26S proteasome-ubiquitin system consists of a protein complex with multiproteolytic activity that degrades ubiquitinated proteins to small polypeptides (2–25 amino acids) (Lecker et al., 2006). In eukaryotes most protein degradation is carried out via the ubiquitin-proteasome pathway. The main functions attributed to this protein degradation system are a rapid degradation of specific proteins that allows cellular adaptation to new environmental conditions, regulation of gene transcription, because many transcription factors are ubiquitinated and degraded by this pathway, a quality control of damaged, misfolded, or denatured proteins, a source of amino acids, and other roles unrelated to proteolysis (Lecker et al., 2006; Nandi et al., 2006). In the Pb-adapted strain, the group of proteins of the ubiquitin-proteasome system whose abundance is higher than that of the control strain (≥ 1.49-fold) constitutes 6.39 % of the total. It consists of 17 proteins compared to the 7 increased in the control. In the Pb-adapted strain, among the enriched proteins (≥ 1.49-fold over the wild type strain) that are involved in the ubiquitin-proteasome system, we found four that are part of the 26S proteasome. The most abundant one (4.2-fold) is the beta-2 subunit (with trypsin-like enzymatic activity), which is essential for the assembly of the 20S proteasome core particle. The detoxification of the insecticide delthamethrin in *Drosophila* is affected by the presence of the beta-2 proteasome subunit, since knockdown of this gene significantly reduces the level of detoxification of this insecticide, and its overexpression increases cell viability (Hu et al., 2016). Among the subunits with proteolytic capacity, subunit 7 (with trypsin-like activity) is also an essential protein for the assembly of the 20S core particle and is also increased (2.79-fold) compared to the control. Two other essential subunits in the assembly of the 20S proteasome particle are the beta-5 and beta-3 subunits, which also appear increased in the Pb-adapted strain but in lower extents (1.21- and 1.14-fold respectively, relative to the control). Beta-5 subunit (with chymotrypsin-like activity) plays a critical role in proteasome-mediated protection against replicative senescence, as overexpression of this subunit increases the resistance of multipotent human bone marrow stromal cells to oxidative stress by hydrogen peroxide (Lu et al., 2014).

Another proteasome component that is abundant in this strain (2.4-fold over the control) is the proteosomal regulatory protein rpn11, which is the only member of the lid (outermost part of the 19S proteasome regulatory particle) with essential catalytic capacity (deubiquitinase) in the proteasome (Verma et al., 2002). Some ATPase proteins associated with different cellular activities (AAA-ATPases) are linked to the proteasome, forming a heterohexameric ring with six distinct subunits (Rpt1–6) (Yedidi et al., 2017). A 26S proteasome ATPase subunit T6 (Rpt6) is also present in the Pb-adapted strain in a level 1.49-fold over the control. The genes encoding the same protein Rpt6 and RPN7 are up-regulated in *T. thermophila* exposed to silver nanoparticles (Piersanti et al., 2021). In contrast, the RPN7 protein (26S proteasome regulatory subunit N7) appears in the control strain (about 2-fold over the Pb-adapted strain). This could mean that silver and lead affect different proteasome subunits.

Proteasome function is regulated by a cyclic AMP-dependent protein kinase (PKA) through phosphorylation of the Rpt6 subunit (Zhang et al., 2007). The Pb-adapted strain presents (1.79-fold relative to the control) a serine/threonine protein kinase (cAMP-dependent kinase or PKA) in the protein-processing functional group (Table 2S), which could phosphorylate the Ser120 residue of RPT6, and it is known that this phosphorylation is responsible for proteasome activation (Wang and Wang, 2020), although it may also be involved in peroxisome biogenesis (Zhao et al., 2014). Other proteins involved in the proteasome function are also present in this strain, such as several non-ATPase regulatory subunits or alpha-type subunits, but in lower levels than 1.49-fold relative to the control (data not shown).

Ubiquitination is a post-translational modification that attaches one or more ubiquitin molecules to a target protein for subsequent degradation in the proteasome. Therefore, it is a fundamental mechanism linked to the proteolytic activity of the proteasome. Three enzymes are required for the binding of ubiquitin to the target protein for degradation; E1 (ubiquitin activation enzyme), E2 (enzyme that conjugates or transports ubiquitin to the target protein) and E3 (ubiquitin-protein ligase, which recognizes the target protein and catalyzes the binding of ubiquitin to that protein) (Lecker et al., 2006). All three types of enzymes are present in the Pb-adapted strain, namely, three isoforms of ubiquitin-conjugating enzyme E2 are shown in 2.74- and 2.09-fold higher levels than the control, two isoforms of E1, one of which is 1.82-fold higher than the control, and only one E3 isoform (1.49-fold).

Other relevant ubiquitin-related proteins present in the Pb-adapted strain are a)- ubiquitin carboxyl-terminal hydrolases which are abundant (144 homologs) in the genome of *T. thermophila*, of which only 6 isoforms were identified in the Pb-adapted strain, one of them is increased 3.17-fold relative to the control, and the rest are below the 1.49-fold threshold. These enzymes have a deubiquitinating function, releasing ubiquitin molecules from the poly-ubiquitin chains of polypeptides, and thus recycling ubiquitin monomers. These enzymes play a crucial role in various cellular processes and oncogenesis (Fang et al., 2010). The gene encoding the human ubiquitin carboxyl-terminal hydrolase L1 is regulated by oxidative stress at both transcriptional and translational levels (Shen et al., 2006). b)- Two isoforms of the HECT-domain ubiquitin-transferase enzyme (a type of ubiquitin protein E3 ligase) (Chen et al., 2017) appear in the Pb-adapted strain, with 2.74- and 2.09-fold increased amounts relative to the control. The levels of these isoforms counterbalance the relatively low amount (1.49-fold) of the above-mentioned E3 ligase, so that the ubiquitin ligase activity of them equals that of the E2 enzyme, thus the ranking of the levels of the three enzymes in the Pb-adapted strain would be E2(6.27-

fold) ≈ E3(6.32-fold) > E1(3.08-fold). The E2 enzyme family is one of the key proteins in the ubiquitin-proteasome system and is linked to the stress response induced by different abiotic agents, as reported in plants, yeast and ciliates. Some examples are as follows: in *Nicotiana tabacum*, overexpression of E2 enzyme NtUBC1 increases resistance against cadmium (Liu et al., 2020); increased expression of LeUBC1 from *Lycopersicon esculentum* is associated with heat-shock stress and Cd chloride toxicity; in *Arabidopsis thaliana*, UBC24/PHO2 is regulated by a microRNA (miR399) that controls inorganic phosphate homeostasis and its mobilization (Bari et al., 2006); ShUbc13 from the ciliate protozoan *Sterkiella histriomuscorum* is involved in the cellular response to DNA damage after UV-irradiation and during the encystment-excystment cycle (Grisvard et al., 2010). c)- Ubiquitin-like modifier-activating enzyme (ATG7) is an E1-like activation enzyme involved in protein lipidation processes and required in membrane fusion events during autophagy and mitophagy that controls the quality and quantity of mitochondria under cellular stress (Lilienbaum, 2013).

4.6. Metallothioneins

In both prokaryotes and eukaryotes, toxic metals induce the appearance of potentially metal(loid)-chelating molecules such as metallothioneins (MT), phytochelatins or glutathione as a mechanism to mitigate their harmful effects on essential proteins or enzymes. In the proteomics analysis of the Pb-adapted strain, the most increased proteins with respect to the control are two metallothioneins (MTs), MTT5 and MTT1 (51.14 and 30.90-fold with respect to the control, respectively), from among the five MT isoforms present in the ciliate genome (Díaz et al., 2007; Gutiérrez et al., 2019). Previous work from our group (De Francisco et al., 2017) has defined *MTT5* as an essential cellular "alarm" gene and is the one that reaches the highest expression levels under the presence of Pb (Díaz et al., 2007; De Francisco et al., 2017; Gutiérrez et al., 2019), although it also responds to Cd and Cu, presenting a good affinity for these metals (Espart et al., 2015). The results of the proteomic analysis in the *T. thermophila* Pb-adapted strain confirm a previous study using quantitative RT-PCR analysis in this same strain, as *MTT5* gene is the one reaching the highest expression levels both in this strain and in the control (De Francisco et al., 2017).

The second place is held by metallothionein MTT1 that likewise corresponds with the previously published gene expression ranking values for the *MTT1* gene in both the Pb-adapted and control strains (De Francisco et al., 2016). MTT1 is preferentially identified as a Cd-MT (Díaz et al., 2007; De Francisco et al., 2017; Gutiérrez et al., 2019), although it can also chelate other metals such as Pb, which is in second place with respect to the induction level of *MTT1* gene expression after 24 h of treatment (De Francisco et al., 2017).

The third and last MT reported in the proteomics analysis of the Pb-adapted strain is MTT2 (3.10-fold increased relative to the control). MTT2 and its paralog MTT4 have been identified as Cu-MTs, as they exhibit their highest affinity for copper (MTT2 > MTT4) (Espart et al., 2015). Therefore, it is unexpected that MTT2 appears in a significant amount in the Pb-adapted strain. One possible explanation is as follows; essential gene *MTT5* is the most induced one under Pb or Cd treatments in all analyzed strains of *T. thermophila* (De Francisco et al., 2017). Based on a previous study about AP-1 transcription factors (bZIP) as potential regulators of MT gene expression in this ciliate (De Francisco et al., 2018a), it was observed that *MTT5* promotes the coordinated differential expression of *MTT1* and *MTT2* under metal stress (MTT1 > > MTT2). This would explain the ranking of MT protein levels (resembling gene expression levels) found under lead stress in the Pb-adapted strain: MTT5 > > MTT1 (about 20-fold the amount of MTT1), MTT1 > > MTT2 (about 28-fold the amount of MTT2). Currently, we do not know the mechanism by which the presence of MTT5 protein triggers the expression of the other two MT genes (*MTT1* and *MTT2*), although MTT1 also chelates Pb (De Francisco et al., 2017, 2018a), or whether MTT2 can also do so.

In some Cd-MT isoforms from several *Tetrahymena* species, Pb leaders the ranking of gene expression induction, depending on the exposure time. (De Francisco et al., 2016). In other organisms such as rats, fish, or humans MTs are also induced by lead (Church et al., 1993; Cheung and Wang, 2005). Lead is the second metal, after Cd, to displace Zn in Zn-MT complexes, or even Cd in Cd-MT complexes (Waalkes et al., 1984; Erk and Raspor, 2001). Transcriptomic analysis of some plants has shown that some MT genes respond equally to Cd and Pb (Kovalchuk et al., 2005).

4.7. Oxidative stress

Metals can directly or indirectly cause oxidative stress due to the formation of reactive oxygen species (ROS). Metals with redox activity (such as Cu, among others) can directly cause ROS by Fenton-Haber-Weiss reactions or auto-oxidation, while metals without redox activity (such as Pb) can indirectly generate oxidative stress by substituting essential cations from biomolecules or by altering antioxidant enzyme activities (glutathione peroxidase, catalase, superoxide dismutase, etc.). Another of the large protein functional groups in the Pb-adapted strain is the one related to oxidative stress (11.27 % of the total proteins), and within the top-ten most abundant proteins of this strain there are two proteins (GPx and Trx) from this group. Glutathione peroxidase (GPx) is the most abundant in the Pb-adapted strain, with almost 21-fold more than the control. It is one of the 12 GPx isoforms present in the *T. thermophila* genome and has been identified as GPX4 or phospholipid hydroperoxide glutathione peroxidase (PHGPx) (Cubas-Gaona et al., 2020). This enzyme protects the cell against lipid peroxidation or H_2O_2 (ROS biochemical indicators) because it can reduce fatty acid hydroperoxides that are esterified to phospholipids, or hydrogen peroxide using glutathione (GSH) as an electron donor (Imai and Nakagawa, 2003). Interestingly, this same GPX4, which appears abundantly in the Pb-adapted strain, also arises in *T. thermophila* exposed to silver nanoparticles (Piersanti et al., 2021), as do two thioredoxin reductases (TTHERM_01222600 and THERM_00142420) (Table 2S), indicating that the response to oxidative stress is common and independent of the metal involved. In the Pb-adapted strain only one other GPx appears, but in an amount lower than 1.49-fold over the control (1.13-fold) and identified as the GPX9 isoform of *T. thermophila*, which is inducible by Pb, as are others from this ciliate such as GPX1, GPX3, GPX10, GPX11 and GPX12 (Cubas-Gaona et al., 2020).

The toxic effect of lead on cell membranes is well known, altering their fluidity and permeability, so that membrane lipid peroxidation is a direct effect of this metal, linked to its neurotoxic effect (Virgolini and Aschner, 2021). In plants, increased lipid peroxidation by Pb treatment is a consequence of high levels of superoxide, hydroxyl radicals and hydrogen peroxide (Kumar and Prasad, 2018). Interestingly, the unique catalase enzyme (CAT1) from *T. thermophila*, which also degrades hydrogen peroxide, was not identified in either the Pb-adapted or the control strains. In leaves and roots of the herbaceous plant *Centella asiatica*, under three different levels of Pb exposure, it is the GPx activity that shows higher values than other antioxidant enzymes, as catalase or superoxide dismutase (Yap et al., 2021).

The second most abundant protein (7.93-fold the control), within the oxidative stress functional group, is a protein with a thioredoxin (Trx) domain. In the Pb-adapted strain, 10 proteins appear to be ascribed to the thioredoxin family, two of which are thioredoxin glutathione reductases (TGR), and all in levels higher than 1.49-fold regarding the control. Two more proteins of this family appear in this strain (one Trx and one TGR) but with values <1.49-fold over the control. Many organisms have two different coexisting antioxidant systems; glutathione (GSH)/glutathione reductase (GR)/glutaredoxin (Grx) and thioredoxin ($Trx(SH)_2$)/thioredoxin reductase (TrxR). Both the GSH tripeptide and the Trx/Grx proteins act as reducing power donors. TGR connects both systems, being able to reduce both Trx and GSH, substituting the functions of TrxR and GR, respectively (Williams et al., 2013). Although in *T. thermophila* there are six genes encoding cytosolic and mitochondrial GR isoforms and four mitochondrial TrxRs, there are in addition five isoforms of TGRs. And three of these seem to be involved in the antioxidant response of the Pb-adapted strain. Thus, this strain should require both Trx and GSH for the defense against the

oxidative stress produced by Pb. The need for GSH under these conditions is evidenced by the presence of a glutathione synthetase (GSH2) in an amount 2.14-fold over the control. In *T. thermophila* there are only two isoforms for this enzyme (GSH1 and GSH2).

Glutathione metabolism is well represented in this Pb-adapted strain, as 5 glutathione-S-transferases (GSTs) are also found with amounts >1.49-fold over the control. Gene expression analysis (by qRT-PCR) of the coding genes of some of these GSTs under metals and other abiotic stressors has been carried out in our research group and confirms their induction under Pb stress. For example, the GST (with a 2.94-fold abundance over the control) is an omega class GST (GSTO4) whose gene expression is induced 3.60-fold relative to the control under Pb stress (950 μM, 24 h treatment) (unpublished data). Interestingly, one of the most overexpressed GSTs (4.3 and 12.1-fold at 2 and 24 h treatment, respectively) under Pb stress (950 μM) measured by qRT-PCR (unpublished data), is an omega GST (GSTO7 or GST61) that does not appear in the Pb-adapted strain. Therefore, this GST would act early after Pb exposure, but it should not have a relevant function in the Pb-adapted strain. Two other GSTs that appear abundant in the control strain; GSTM49 (mu class) (2.06-fold) and GSTN2 (unclassified) (1.88-fold) (Fig. 2S), were also quantified by qRT-PCR in the presence of Pb, and both gave a negative result (no induction under Pb stress) (unpublished data), thus confirming the proteomics results. Several genes encoding GSTs are also up-regulated under stress caused by silver nanoparticles or $AgNO_3$ (Piersanti et al., 2021).

Another key antioxidant enzyme involved in the conversion of superoxide ion into hydrogen peroxide, which will be subsequently degraded by glutathione peroxidase, is superoxide dismutase (SOD), and in fact an iron/manganese SOD also appears increased in the Pb-adapted strain (3.28-fold more than the control).

Many of the lead-toxic effects in mammals are based on the production of oxidative stress which induces an imbalance of cellular antioxidant agents that is resolved by increasing the presence of similar antioxidant agents (SOD, GPx, GST, GSH, etc.) in many organisms (Singh et al., 2018). In the yeast *Papiliotrema laurentii*, which precipitates Pb in the ClPm form, it increases the enzymatic activity of SOD and catalase, relative to control or exposure with other metal(loid)s (Sarkar et al., 2019). OsmC and Ohr constitute two subfamilies of proteins, present in both prokaryotes and eukaryotes, with thiol-dependent peroxidase activity and with the ability to reduce organic hydroperoxides (Meireles et al., 2017). This peroxidase activity may be related to the detoxification of endogenously originated hydroperoxides and to exogenous oxidative stress as occurs in bacteria (Meireles et al., 2017). Among the five OsmC protein isoforms encoded by the *T. thermophila* macronuclear genome, three of them are detected in the Pb-adapted strain (Table 2S), and only one of them (TTHERM_00640030) has been also reported in *T. thermophila* exposed to silver nanoparticles (Piersanti et al., 2021). These results reveal for the first time in eukaryotic microorganisms that the peroxidase activity of OsmC-type enzymes is involved in metal-induced oxidative stress.

Truncated hemoglobins are proteins found in bacteria, eukaryotic microorganisms, and plants, and have been implicated in tolerance to nitrosative stress (Angelo et al., 2008). This type of stress consists of a nitric oxide (NO)-mediated nitrosylation of redox-sensitive thiols, involved in processes of signal transduction, gene expression, cell growth and apoptosis. Reactive oxygen species (ROS) and nitrogen species (RNS) can originate from endogenous or exogenous inducers. Pb induces both oxidative and nitrosative stress, as observed in human oral mucosal cells (Wannhoff et al., 2013). Therefore, in the Pb-adapted strain a nitrosative stress could originate by an increase in NO, and although this gaseous molecule can protect the cell against oxidative stress caused by Pb (Kaur et al., 2015), an intracellular excess of NO could trigger the protective action of truncated hemoglobin. Truncated hemoglobin from *T. pyriformis* is essential in NO detoxification (Igarashi et al., 2011). The *T. thermophila* Pb-adapted strain exhibits three isoforms, one of them (4.99-fold over the control) referred to as HEM1, and two others yet to be named. The gene encoding this same protein (HEM1), together with the gene encoding another group 1 truncated hemoglobin (THERM_00439070), also present in the Pb-adapted strain, are up-regulated under the stress of silver nanoparticles or silver nitrate (Piersanti et al., 2021).

4.8. Vesicle trafficking and exocytosis

We can draw a coherent scenario of vesicle trafficking that could be involved both in autophagy-lysosomal proteolytic processes and/or in the formation of vesicles with the electrodense bodies identified as ClPm. Due to the complexity of this process, we have elaborated a scheme (Fig. 10) for a better understanding, where all the proteins from both functional groups present in the Pb-adapted strain are included.

Clathrin is a protein that forms a type of vesicular coat. Upon assembly of three heavy and three light chains of this protein, a truncated icosahedral structure is formed around the budding vesicle membrane (McMahon and Mills, 2004). Associated with clathrin are clathrin adaptor proteins (AP) (also known as adaptins) that attach the clathrin coat to the vesicle membrane and are responsible for vesicle cargo selection and transport. There are several types of AP complexes, among them AP1 is involved in the transport of lysosomal enzymes between the Trans-Golgi network (TGN) and endosomes (Nakatsu et al., 2014). The protein dynamin is located at the base of the clathrin-coated vesicles and promotes vesicle fission and release from the Golgi (Elde et al., 2005). Some of these proteins are shown in the Pb-adapted strain in increased levels >1.49-fold relative to the control, as clathrin light chain, APM1B clathrin adapter, dynamin protein and dynamin GTPase (Table 4S, [1] in Fig. 10), while other APs appear at amounts <1.49-fold relative to the control such as clathrin heavy chain, and clathrin adapter AP1 (mu and beta subunits). The HVA22/TB2/DP1 family protein is involved in the organization of the endoplasmic reticulum (ER) and regulation of vesicular trafficking. In plants, they are induced by various environmental stressors, such as dehydration, salinity, elevated temperature, etc. (Brands and Ho, 2002; Gomes-Ferreira et al., 2019). The lead-adapted strain expresses one of the four isoforms of this protein in *T. thermophila*, about 3-fold over the control strain ([2] in Fig. 10, Table 4S). Vacuolar protein sorting-associated proteins (Vps) are related to multivesicular bodies (MVB) or late endosomes (LE) and have an essential function in recycling of components of the ESCRT-III complex (endosomal sorting complexes required for vesicular transport) by directing the excision of vesicles into the endosomal organelle (Schöneberg et al., 2016). Three of these proteins, Vps4b, Vps33 and Vps29, the latter at <1.49-fold over the control, are present in the Pb-adapted strain (Tables 2S and 4S). Vps4 functions as a hexamer, with a microtubule interaction and transport domain and a catalytic AAA+ ATPase domain, while Vps33 binds SNARE (Soluble NSF (N-ethylmaleimide-sensitive factor) Attachment protein [SNAP] Receptors) domains (which mediate vesicle fusion) and Vps29 is required for recycling Vps10 from the pre-vacuolar endosome (VPE) to the Golgi ([3] in Fig. 10).

Eight proteins belonging to the Ras superfamily of small GTPases are detected in the Pb-adapted strain. Rab GTPases regulates various stages of membrane trafficking, including vesicle formation and mobility along actin and tubulin microfilaments (Homma et al., 2021). Three different Rab proteins are abundant in the Pb-adapted strain, namely RAB2, RAB7 and RAB8B, while RAB6A appears in levels <1.49-fold relative to the control ([4] in Fig. 10). In addition, two Rab GDP dissociation inhibitor (GDI1) homologs appear in this strain at higher levels than the control (Table 4S). Proteins involved in vesicular trafficking, such as Rab, are physically translocated from the donor to the target compartment and recycled from the target to the donor compartment by means of a chaperone (GDP-dissociation inhibitor or GDI) that facilitates their release from the target compartment (Tuvim et al., 2001).

Vacuolar H^+ ATPases (V-ATPases) are primary proton pumps that acidify various types of eukaryotic cellular compartments (such as vacuoles) and are involved in vital intra- and intercellular processes such as receptor-mediated endocytosis, protein trafficking, active transport of metabolites, homeostasis, and neurotransmitter release (Beyenbach and Wieczorek, 2006). Four V-ATPases or vacuolar-ATP synthases appear in the Pb-adapted strain, two of them in amounts >1.49-fold over the control

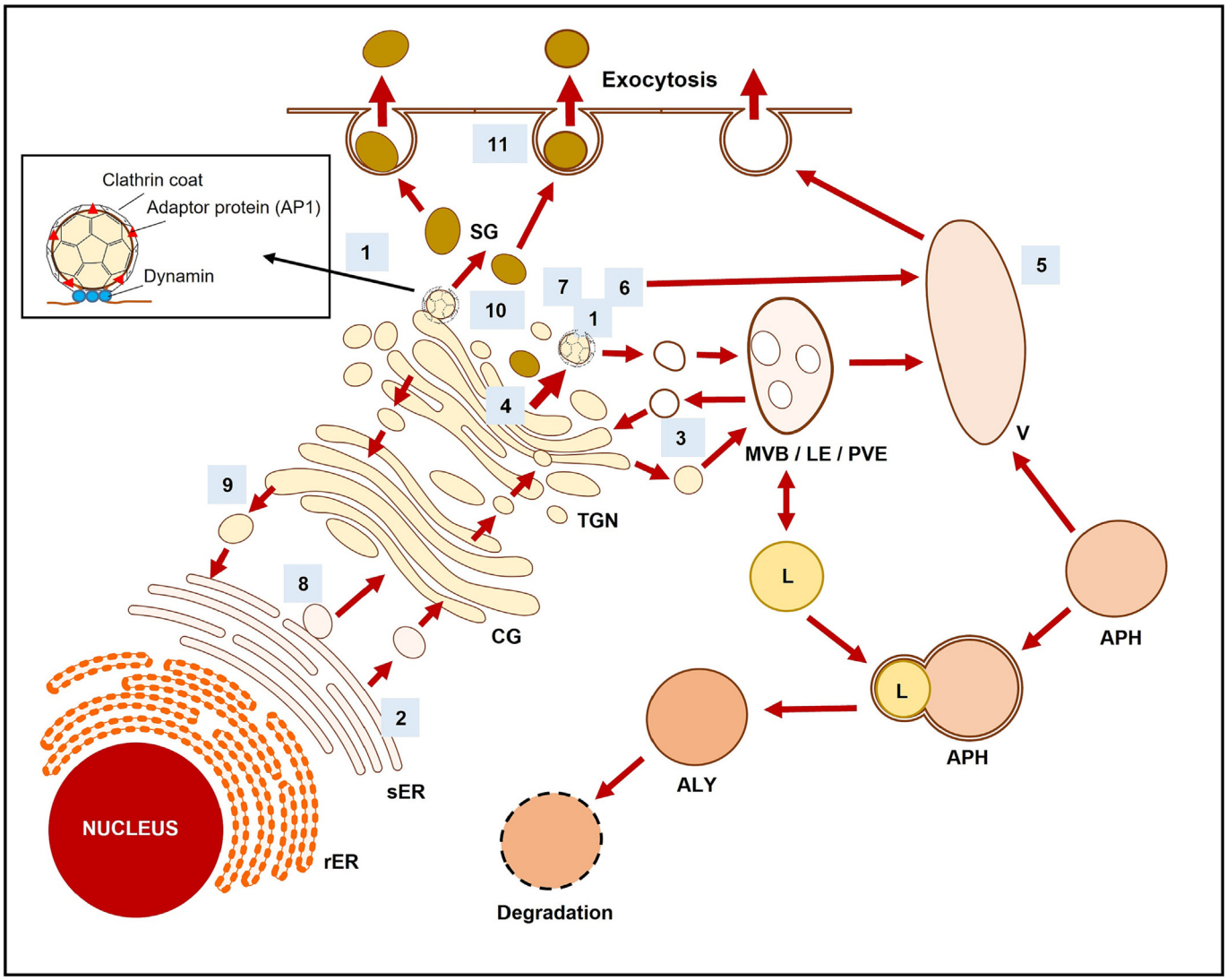

Fig. 10. Scheme showing the main proteins involved in vesicular trafficking and exocytosis present in the Pb-adapted strain. Each number has its explanation in the text. rER (rough endoplasmic reticulum). sER (smooth endoplasmic reticulum). CG (Cis-Golgi). TGN (Trans-Golgi network). MVB (multivesicular bodies). LE (late endosomes). PVE (pre-vacuolar endosome). SG (secretory granule). V (vacuole). APH (autophagosome). L (lysosome). ALY (autofagolisosome).

(Table 2S) and two others in lower levels (Table 4S). These enzyme complexes could be located either in the membranes of vacuoles, endosomes, lysosomes, or the cytoplasmic membrane ([5] in Fig. 10). Aluminum-resistant wheat overexpressing a V-ATPase has been reported (Hamilton et al., 2001), and for these authors it means an adaptation to aluminum stress.

One possible route of vacuolar protein transport is from the ER to the Golgi and then to the trans-Golgi network (TGN), and from there to a pre-vacuolar compartment (PVC) (Fig. 10). This protein trafficking requires numerous protein factors, one of which is the vacuolar sorting receptor (VSR) (Kang and Hwang, 2014). At the TGN, the VSR recognizes the protein cargo and VSR-cargo complexes are packaged into clathrin-coated vesicles from the TGN ([6] in Fig. 10). These vesicles fuse with the PVC and VSR releases the cargo inside. The PVC after maturation can give rise to a lytic vacuole (Kang and Hwang, 2014). *T. thermophila* has two isoforms of this protein (VSR), one of which is shown (1.85-fold over the control) in the Pb-adapted strain (Tables 2S, 4S). Dynamitin is a subunit of the multiprotein complex dynactin, required for the microtubular motor dynein. The dynein-dynactin complex is involved in vesicular transport among other possible functions (Liu, 2017). This subunit appears in the Pb-adapted strain (Tables 2S and 4S) as a component of the system that facilitates vesicle or secretory granule mobility through the cytoplasm ([7] in Fig. 10).

Eukaryotic cells have a series of cytoplasmic coat proteins (COPs) that are incorporated (as protein complexes) into the Golgi or ER membranes to form vesicular coatings. There are two types of COP-type vesicular coatings: COP-I and COP-II (Duden, 2003). COP-II coatings form vesicles that transport proteins newly synthesized in the ER and transfer them to the cis-Golgi system. COP-I form vesicles that selectively recycle proteins and perform reverse or retrograde transport from the cis-Golgi to the ER (Lee and Goldberg, 2010) ([8 and 9] in Fig. 10). Components of both types of vesicle coatings have been identified in the Pb-adapted strain (Tables 2S and 4S). From the COP-II complex there are two isoforms of the Sec23 complex plus an ADP-ribosylation factor small GTPase (Sar1), whereas from the COP-I complex there are five different subunits (alpha, beta, gamma (two isoforms) and delta) of the seven presents in the coatomer complex. *T. thermophila* has 20 isoforms of the coatomer gamma subunit. COP-II has a Sec13 protein complex, which interestingly appears as a Sec13 transporter protein in the control strain with a 5.40-fold abundance relative to the Pb-adapted strain (Table 3S). Thus, due to its abundance in the control, a higher amount is not required in the Pb-adapted strain to form a functional Pb-POP-II complex.

Two isoforms of SCAMP (secretory carrier membrane proteins) are present in the genome of *T. thermophila*, only one of which appears in the Pb-adapted strain (Tables 2S and 4S). These membrane proteins constitute a

family and are involved in exocytosis processes (recycling of exocytic vesicles from the outside to different cellular compartments, endosomes, trans-Golgi vesicles, secretory granules, etc.) (Hubbard et al., 2000; Law and Jiang, 2012) ([10] in Fig. 10). In the functional group secretory granules (SG) (exocytosis) of the Pb-adapted strain, six proteins identified as granule lattice proteins are shown, namely GRL5, GRL7, GRL8, GRL4 (>1.49-fold relative to control), GRL1 and GRL3 (in amounts <1.49-fold the control). Nine GRL isoforms are present in the genome of *T. thermophila*, but only six of them (GRL1, 3, 4, 5, 7 and 8) appear to be essential in the formation of dense core granules (Cowan et al., 2005), and these six proteins are present at substantial levels in the Pb-adapted strain. Dense nucleoid granules are defined as specialized vesicles for storing highly concentrated proteins, which can be excreted out of the cell via exocytosis across the cytoplasmic membrane (Cowan et al., 2005; Rahaman et al., 2009). In addition to these GRL proteins that form the crystalline lattice of the dense core granules (extrusomes) or extrusion organelles, the Pb-adapted strain shows increased levels (1.85-fold over the control strain) of a second class of proteins (granule-tip1 or GRT1) involved in the formation of the extrusome tip domain that facilitates fusion with the cytoplasmic membrane, and appears to have a post-exocytotic function (Rahaman et al., 2009) (Table 4S, [11] in Fig. 10). All these proteins are part of the extrusomes known as mucocysts in *T. thermophila*, but remarkably these organelles are not observed in the Pb-adapted strain, unlike the control, by transmission electron microscopy analysis. Could they be involved in the aggregation, condensation, and crystallization (biomineralization) of pyromorphite in vesicles containing this mineral, which are subsequently expelled by exocytosis? Another possibility is that due to the high traffic of vesicles or vacuoles expelling pyromorphite deposits outside the cell, the normal mucocyst extrusion was altered in this Pb-adapted strain, and consequently higher amounts of proteins involved in mucocyst formation and extrusion are produced, though they may not be formed and anchored to the ciliate pellicle.

Due to the substantial length of the article and especially the Discussion section, we have moved the sections analyzing stress proteins, lipid metabolism, energy metabolism, transmembrane transport proteins and signaling, and other proteins abundant in the Pb-adapted strain to the supplementary material, together with the references cited in these sections (see Text-2S).

4.9. Lead biomineralization to chloropyromorphite

Biomineralization involves living organisms (macro or microorganisms) capable of transforming soluble toxic metals into less toxic insoluble compounds, as a defense mechanism against the toxic metal present in the environment. This process can occur extracellularly as the organism excretes molecules that facilitate metal mineralization, or intracellularly by inducing mineralization inside the cell, accumulating it, and subsequently excreting it outside the cell (Kirsch, 2012). As already indicated in the introduction, both prokaryotes and eukaryotes can perform a lead biomineralization originating different compounds, and among them the most common is pyromorphite (a highly insoluble lead phosphate mineral). However, although pyromorphite formation has been described in several organisms (bacteria, fungi, yeasts, and nematodes), the molecular and physiological elements involved in both extracellular and, much more, intracellular biomineralization processes are still unknown.

In soil, pyromorphite formation is favored by the presence of protonated phosphate species (H_3PO_4 and $H_2PO_4^-$), therefore a low (acidic) pH is required to induce the transformation of Pb to chloropyromorphite ($Pb_5[PO_4]_3Cl$) (Scheckel et al., 2013). The current hypothesis, supported by some experimental results, regarding the microbial lead-biomineralization to pyromorphite and its precipitation outside/inside of the cell, is based on the production of extra- or intracellular phosphatases that release phosphate from different organic sources (Gadd et al., 2012; Liang et al., 2016; Jiang et al., 2020). Nothing is known about the effect of this increased phosphatase activity on the physiology of the microorganism, mainly when intracellular phosphatases are involved, nor what are the real phosphate compounds on which the enzyme acts. Different possible sources of phosphate, either inorganics as polyphosphates and pyrophosphate, or organics, such as glycerophosphate, phospho-monoesters, −diesters or -triesters, inositol phosphate, etc., have been suggested (Liang et al., 2016; Jiang et al., 2020). It has also been proposed that some of these phosphate sources could be present either in the cytoplasm or in vacuoles (like polyphosphate in yeasts) (Okorokov et al., 1980).

In the lead-adapted strain, 22 proteins with a phosphatase domain (Table 5S) versus 21 with kinase or phosphorylase domains are recorded, regardless of their abundance values (> or < 1.49-fold) compared to the control; while in the control strain these protein sets are quite similar; 20 with phosphatase domain (Table 6S) and 21 with kinase or phosphorylase domains (data not shown). The histidine phosphatases superfamily, which dephosphorylate phosphorylated histidine residues present in many different proteins, contains two branches or clades and they have a wide variety of functions (Rigden, 2008; Klumpp and Krieglstein, 2009). In the Pb-adapted strain, at least six protein phosphatases are detected which would fall into one of the two clades of this superfamily. There are two enzymes from the histidine phosphatase family that belong to clade 1, one of which is the most abundant phosphatase in this strain (3.54-fold over the control). A fructose-1,6-bisphosphatase (2.64-fold over the control) (Table 5S) also belongs to this clade 1. These enzymes are usually cytosolic (Rigden, 2008). Two other proteins identified as belonging to the histidine phosphatase family belong to clade 2, which are present in smaller amounts (1.32 and 1.10-fold over the control) (Table 5S). The last one is the lysosomal acid phosphatase LAP1 from *T. thermophila*. In addition, a protein from the inositol monophosphatase family (1.49-fold over the control) is also included in clade 2. These clade 2 phosphatases are usually located in lysosomes, endosomal vesicles, ER, cytoplasmic membrane, and some may be excreted to the extracellular environment (Rigden, 2008).

The serine/threonine protein phosphatases superfamily includes phosphoprotein phosphatases (PPP) that dephosphorylate phosphorylated serine/threonine residues of different proteins (Klumpp and Krieglstein, 2002). The Pb-adapted strain presents seven protein phosphatases included in this family, being the most abundant (1.59-fold over the control) one just defined as serine/threonine protein phosphatase (Table 5S), and others, in lower abundance with respect to the control, identified as protein phosphatases 4 (PPP4) and 2C (PPP2C). These phosphatases may be involved in many essential biological functions, such as signaling, autophagy, protein processing, cell cycle regulation, and DNA replication, among others (Wera and Hemmlngst, 1995; Klumpp and Krieglstein, 2002).

The Pb-adapted strain also presents an inosine triphosphate pyrophosphatase (1.88-fold over the control) (Table 5S), which hydrolyzes non-canonical purine nucleotides (such as inosine triphosphate among others), thus excluding the incorporation of these non-canonical nucleotides into DNA or RNA, thus preventing lesions or mutations in these macromolecules (Zamzami, 2022). This enzyme releases pyrophosphate or diphosphate, which subsequently, by the concourse of an inorganic pyrophosphatase (PPase) activity, can be a possible pathway for the intracellular generation of phosphate ions. There are two main types of inorganic pyrophosphatases, soluble (cytosolic and organellar sPPases) and membrane-integral or vacuolar H^+-translocating pyrophosphatases (H^+-PPases) (Pérez-Castiñeira et al., 2001, 2002; Holmes et al., 2019). According to the information currently available in databases, the genome of *T. thermophila* encodes four sPPases, three of them with N-terminal extensions, and six membrane H^+-PPases. Two of the latter (TTHERM_00059370 and TTHERM_00392790 genes) should not be bona fide H^+-PPases as key lack the DN/LVGDNVG catalytic motif which is present in all membrane PPases described so far (Holmes et al., 2019); furthermore, two other contiguous genes of this group (TTHERM_000773801 and TTHERM_000773802) encode the N- and C-terminal regions of a single PPase protein, so this protist must have actually three genes encoding H^+-PPases (unpublished results). Among them the Pb-adapted strain presents only one cytosolic sPPase (with no N-terminal extended region) in slightly higher abundance relative to the control (1.05-fold) (Table 5S), while the control strain presents four PPases at higher levels compared to the Pb-adapted strain, two vacuolar H^+-PPases and two sPPases, the latters with N-terminal extensions suggesting organelle targeting (Table 6S).

Most of these enzymes release phosphate regardless of whether it is incorporated into the general metabolism or used in the Pb-adapted strain to form intracellular pyromorphite. And with respect to where and how this pyromorphite might originate and accumulate into the cell, the following scenario may be considered: The intense vesicular traffic in the Pb-adapted strain reflects the significant vesiculation involved in the inclusion and deposition of chloropyromorphite nanoparticles. Extracellular lead could be incorporated into the cytoplasm by different transporters (such as MFS transporters or those that are improperly used by toxic metals as P-type ATPases), then accumulate in vacuoles by similar transport mechanisms. The abundant vacuolar-H^+-ATPases in this strain can acidify the vacuole lumen, thus creating an acidic luminal medium. Both PPi and Pi, as is assumed to occur in acidocalcisomes, could be transported from the cytosol to inside vacuoles by presumed specific transporters as vacuolar transporter chaperone (VTC) complex (Lander et al., 2016). However, no gene encoding this type of proteins has been identified in the genome of *T. thermophila*. Another possibility for the incorporation of phosphate into the vacuole, supported by proteomic analysis, would be the existence of START domain-containing proteins, which are very abundant in the Pb-adapted strain (Table 2S). These proteins can transport phospholipids across membranes of different cellular compartments (such as vacuoles). After incorporation into the vacuole, phospholipids could be digested by enzymes from the patatin phospholipase family, also abundant in this strain (Table 2S). The sequences of both phospholipases, present in the Pb-adapted strain, have signal peptides at their N-terminal ends, so their localization could be vacuolar. To release phosphate, a phospholipase C should hydrolyze the ester bond between the glycerol and phosphate groups of the phospholipid (Sekiya, 2013). In plants, these phospholipases play an important role in the cellular response to biotic and abiotic stressors (Hong et al., 2016; Ali et al., 2022). In this way, inside the vacuole there would be an acidic medium and a phosphate source to which the lead would bind to form pyromorphite. The accumulation and precipitation of this mineral inside the vacuole would favor crystallization by molecular crowding.

Polyphosphate could be another possible source of phosphate, but this proteomic study has not identified any enzymes involved in the degradation of vacuolar polyphosphates, such as the PPX1-type exopolyphosphatases found in fungi. In addition, polyphosphates (as inorganic polyanions) can chelate or sequester metal cations, and thus decrease the toxic effect of certain metals on essential proteins (Albi and Serrano, 2016). Pb(II), among other metal cations, can be sequestered by polyphosphate (Keasling et al., 1998). However, in the *T. thermophila* Pb-adapted strain, we have no evidence that polyphosphate can be an important element in the stress response to lead; on the contrary, it is metallothioneins (mainly MTT5 and MTT1) that are involved in lead chelation as a first line defense mechanism.

5. As a conclusion: an integrated model of the stress response to lead in the Pb-adapted strain

Fig. 11 summarizes the main and most credible processes that we believe may be involved in the stress response of a *T. thermophila* strain adapted over time to increasing lead concentrations. This model includes 12 main elements or aspects, numbered from 1 to 12 in Fig. 11, which are briefly commented as follows: 1- Lead could enter the cell through P type-ATPase transporters, either specific for heavy metals or parasitizing

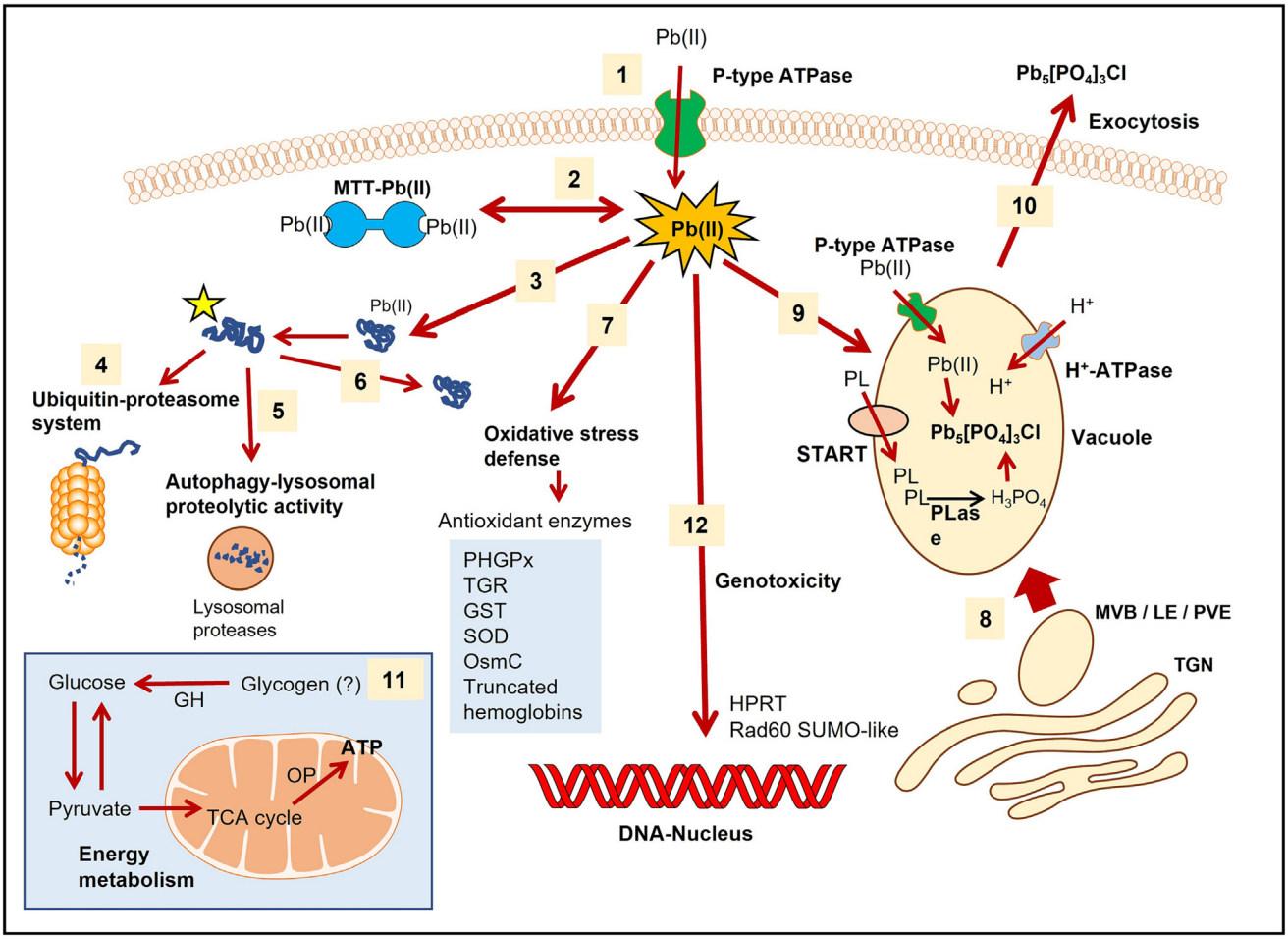

Fig. 11. Scheme of the model integrating the main elements and processes that presumably take place in the Pb-adapted strain in response to extreme Pb-induced stress. Each number has its explanation in the text. MTT-Pb(II) (metallothionein-Pb complex). PL (phospholipid). PLase (phospholipase). TGN (Trans-Golgi network). MVB (multivesicular bodies). LE (late endosomes). PVE (pre-vacuolar endosome). GH (glycosyl hydrolase). OP (oxidative phosphorylation). For further explanation, see text.

one used for essential metals. 2- A first defense mechanism often used by *T. thermophila* to detoxify toxic metals is the use of metallothioneins (Gutiérrez et al., 2019), in this case mainly MTT5 and MTT1 isoforms. This would inactivate an important amount of Pb(II), minimizing its potential toxicity. 3- However, and probably due to the high extracellular lead concentration to which the Pb-adapted strain is exposed, it is not sufficient to prevent the cellular toxic effects of this metal. High proteotoxicity is one of the deleterious effects of lead as it triggers intense proteolytic processes. 4- The ubiquitin-proteasome system is strongly involved in the breakdown of defective proteins caused by Pb(II). 5- In addition, other proteolytic activities by lysosomal enzymes seem to be involved in the destruction of defective proteins, and in both cases (4 and 5) the released amino acids can be reused in new protein synthesis necessary for the stress response developed by this strain. 6- A whole set of stress proteins would be involved in the correct folding of many Pb(II) misfolded proteins to become functional again. 7- Like other toxic metals, lead induces high cellular oxidative stress, which triggers a whole set of antioxidant enzymes to mitigate the oxidative effect caused by ROS formation. 8- One of the most remarkable and novel cell biological effects showed by the Pb-adapted strain is the induction of high levels of vesicular trafficking. Multivesicular bodies (MVB) and prevacuolar endosomes (PVE) can originate from the TGN and eventually give rise to vacuoles. In the Pb-adapted strain, ClPm has been detected in vacuoles or vesicles, and could form, precipitate, and crystallize inside them. 9- A number of elements can be envisaged that could facilitate the lead-biomineralization process, which could be at least four: a metal P-type-ATPase that will incorporate Pb (II) into the vacuole, a H^+-ATPase pump that will acidify the vacuolar lumen, a START protein complex that will transport phospholipids into the vacuole and a phospholipase that will release phosphate from the phospholipid molecules. This is a proposal elaborated from some proteomic data, although we recognize that other hypotheses are possible. 10- Finally, the aggregates of ClPm nanoparticles would be excreted outside of the cell by exocytosis. 11- Probably, the energetic metabolism linked to all detoxification processes present in the Pb-adapted strain should be considerably high. The cell requires sufficient carbon and energy sources to generate high ATP levels, which could be glycogen or another polysaccharide. Enzymes for glycolysis, gluconeogenesis, the TCA cycle, and oxidative phosphorylation are well represented in the proteomic data of the Pb-adapted strain, indicating that the cell synthesizes enough ATP to maintain its adaptation to lead. 12- Finally, lead can also produce some genotoxicity, so the Pb-adapted strain must also repair the DNA altered by exposure to this metal. Both the HPRT enzyme and Rad60 SUMO-like protein, abundant in the Pb-adapted strain, may be involved in the recovery of purine bases from degraded DNA and in DNA repair and recombination processes (Boyd et al., 2010).

CRediT authorship contribution statement

P.dF, F.A, A.M-G, and J.C.G designed and performed the experiments; P. dF, A.S, and J.C.G analyzed the data; J.C.G wrote the manuscript, conceptualized and supervised the study, and acquired funding; P.dF, F.A, A.M-G, A. S, and J.C.G reviewed literature and critically discussed the manuscript draft version. All authors have read and approved the final version of the manuscript.

Data availability

Data will be made available on request.

Declaration of competing interest

The authors declare that they have no competing interests.

Acknowledgements

Work carried out in this study was funded by the Spanish Ministry of Economy and Competitiveness, grant number CGL2016-75494-R awarded to J.C.G.

Appendix A. Supplementary data

Supplementary data to this article can be found online at https://doi.org/10.1016/j.scitotenv.2023.164252.

References

Albi, T., Serrano, A., 2016. Inorganic polyphosphate in the microbial world. Emerging roles for a multifaceted biopolymer. World J. Microbiol. Biotechnol. 27, 1–12. https://doi.org/10.1007/s11274-015-1983-2.

Albiston, A.L., Ye, S., Chai, S.Y., 2004. Membrane bound members of the M1 family: more than aminopeptidases. Protein Pept. Lett. 11, 491–500. https://doi.org/10.2174/0929866043406643.

Ali, U., Lu, S., Fadlalla, T., Iqbal, S., Yue, H., et al., 2022. The functions of phospholipases and their hydrolysis products in plant growth, development, and stress responses. Prog. Lipid Res. 86, 1–18. https://doi.org/10.1016/j.plipres.2022.101158.

Angelo, M., Hausladen, A., Singel, D.J., Stamler, J.S., 2008. Interactions of NO with hemoglobin: from microbes to man. In: Robert Poole, R.K. (Ed.), Methods in Enzymology. 436. Academic Press-Elsevier, pp. 131–168. https://doi.org/10.1016/S0076-6879(08)36008-X.

Baker-Austin, C., Wright, M.S., Stepanauskas, R., McArthur, J.V., 2006. Co-selection of antibiotic and metal resistance. Trends Microbiol. 14, 176–182. https://doi.org/10.1016/j.tim.2006.02.006.

Bari, R., Pant, B.D., Stitt, M., Scheible, W.-R., 2006. PHO2, microRNA399, and PHR1 define a phosphate-signaling pathway in plants. Plant Physiol. 141, 988–999. https://doi.org/10.1104/pp.106.079707.

Beyenbach, K.W., Wieczorek, H., 2006. The V-type H+ ATPase: molecular structure and function, physiological roles and regulation. J. Exp. Biol. 209, 577–589. https://doi.org/10.1242/jeb.02014.

Bizo, M.L., Nietzsche, S., Mansfeld, U., Langenhorts, F., Majzlan, J., et al., 2017. Response to lead pollution: mycorrhizal *Pinus sylvestris* forms the biomineral pyromorphite in roots and needles. Environ. Sci. Pollut. Res. 24, 14455–14462. https://doi.org/10.1007/s11356-017-9020-7.

Boyd, L.K., Mercer, B., Thompson, D., Main, E., Watts, F.Z., 2010. Characterization of the SUMO-like domains of *Schizosaccharomyces pombe* Rad60. PLoS One 5 (9), e13009. https://doi.org/10.1371/journal.pone.0013009 1-11.

Brands, A., Ho, T.H., 2002. Function of a plant stress-induced gene, HVA22. Synthetic enhancement screen with its yeast homolog reveals its role in vesicular traffic. Plant Physiol. 130, 1121–1131. https://doi.org/10.1104/pp.007716.

Burgos, A., Maldonado, J., De los Rios, A., Sole, A., Esteve, I., 2013. Effect of copper and lead on two consortia of phototrophic microorganisms and their capacity to sequester metals. Aquat. Toxicol. 140-141, 324–336. https://doi.org/10.1016/j.aquatox.2013.06.022.

Chen, Z., Jiang, H., Xu, W., Li, X., Dempsey, D.R., et al., 2017. A tunable brake for HECT ubiquitin ligases. Mol. Cell 66, 345–357. https://doi.org/10.1016/j.molcel.2017.03.020.

Cheung, M., Wang, W.-X., 2005. Influence of subcellular metal compartmentalization in different prey on the transfer of metals to a predatory gastropod. Mar. Ecol. Prog. Ser. 286, 155–166.

Church, H.J., Day, J.P., Braithwaite, R.A., Brown, S.S., 1993. Binding of lead to a metallothionein-like protein in human erythrocytes. J. Inorg. Biochem. 49, 55–68. https://doi.org/10.1016/0162-0134(93)80048-e.

Clipson, N., Gleeson, D.B., 2012. Fungal biogeochemistry: A central role in the environmental fate of lead. Curr. Biol. 22, R82–R84. https://doi.org/10.1016/j.cub.2011.12.037.

Cowan, A.T., Bowman, G.R., Edwards, K.F., Emerson, J.J., Turkewitz, A.P., 2005. Genetic, genomic, and functional analysis of the granule lattice proteins in *Tetrahymena* secretory granules. Mol. Biol. Cell 16, 4046–4060. https://doi.org/10.1091/mbc.e05-01-0028.

Cubas-Gaona, L.L., De Francisco, P., Martin-González, A., Gutiérrez, J.C., 2020. *Tetrahymena* glutathione peroxidase family: A comparative analysis of these antioxidant enzymes and differential gene expression to metals and oxidizing agents. Microorganisms. 8, 1–23. https://doi.org/10.3390/microorganisms8071008.

De Francisco, P., Melgar, L.M., Díaz, S., Martín-González, A., Gutiérrez, J.C., 2016. The *Tetrahymena* metallothionein gene family: twenty-one new cDNAs, molecular characterization, phylogenetic study, and comparative analysis of the gene expression under different abiotic stressors. BMC Genomics 17 (346), 1–23. https://bmcgenomics.biomedcentral.com/articles/10.1186/s12864-016-2658-6.

De Francisco, P., Martin-González, A., Turkewitz, A.P., Gutiérrez, J.C., 2017. Extreme metal adapted, knockout and knockdown strains reveal a coordinated gene expression among different *Tetrahymena thermophila* metallothionein isoforms. PLoS One 12 (12), e0189076. https://doi.org/10.1371/journal.pone.0189076 1–23.

De Francisco, P., Amaro, F., Martin-González, A., Gutiérrez, J.C., 2018a. AP-1 (bZIP) transcription factors as potential regulators of metallothionein gene expression in *Tetrahymena thermophila*. Front. Genet. 9 (459), 1–20. https://doi.org/10.3389/fgene.2018.00459.

De Francisco, P., Martin-González, A., Turkewitz, A.P., Gutiérrez, J.C., 2018b. Genome plasticity in response to stress in *Tetrahymena thermophila*: selective and reversible chromosome amplification and paralogous expansion of metallothionein genes. Environ. Microbiol. 20, 2410–2421. https://doi.org/10.1111/1462-2920.14251.

Díaz, S., Martin-González, A., Gutiérrez, J.C., 2006. Evaluation of heavy metal acute toxicity and bioaccumulation in soil ciliated protozoa. Environ. Int. 32, 711–717. https://doi.org/10.1016/j.envint.2006.03.004.

Díaz, S., Amaro, F., Rico, D., Campos, V., Benítez, L., et al., 2007. Tetrahymena metallothioneins fall into two discrete subfamilies. PLoS One 2 (3), 1–14. https://doi.org/10.1371/journal.pone.0000291 e29.

Dubicka, Z., Gorzelak, P., 2017. Unlocking the biomineralization style and affinity of paleozoic fusulinid foraminifera. Sci. Report. 7, 15218. https://doi.org/10.1038/s41598-017-15666-1.

Duden, R., 2003. ER-to-Golgi transport: COP I and COP II function (review). Mol. Membr. Biol. 20, 197–207. https://doi.org/10.1080/0968768031000122548.
Dunlop, S., Chapman, G., 1981. Detoxication of zinc and cadmium by the freshwater protozoan *Tetrahymena pyriformis*: II. Growth experiments and ultrastructural studies on sequestration of heavy metals. Environ. Res. 24, 264–274. https://doi.org/10.1016/0013-9351(81)90156-0.
Eisen, J.A., Coyne, R.S., Wu, M., Wu, D., Thiagarajan, M., et al., 2006. Macronuclear genome sequence of the ciliate *Tetrahymena thermophila*, a model eukaryote. PLoS Biol. 4 (9), e286. https://doi.org/10.1371/journal.pbio.0040286.
Elde, N.C., Morgan, G., Winey, M., Sperling, L., Turkewitz, A.P., 2005. Elucidation of clathrin-mediated endocytosis in *Tetrahymena* reveals an evolutionarily convergent recruitment of dynamin. PLoS Genet. 1 (5), e52. https://doi.org/10.1371/journal.pgen.0010052 0514-0526.
Erk, M., Raspor, B., 2001. Interference of Pb leaching from the pH electrode on Cd-metallothionein complex. Anal. Chim. Acta. 442, 165–170.
Espart, A., Marín, M., Gil-Moreno, S., Palacios, O., Amaro, F., et al., 2015. Hints for metal-preference protein sequence determinants: different metal binding features of the five *Tetrahymena thermophila* metallothioneins. Int. J. Biol. Sci. 11, 456–471. https://doi.org/10.7150/ijbs.11060.
Fang, Y., Fu, D., Shen, X.-Z., 2010. The potential role of ubiquitin c-terminal hydrolases in oncogenesis. Biochim. Biophys. Acta 1806, 1–6. https://doi.org/10.1016/j.bbcan.2010.03.001.
Fernández-Leborans, G., Olalla Herrero, Y., Novillo, A., 1998. Toxicity and bioaccumulation of lead in marine protozoa communities. Ecotoxicol. Environ. Saf. 39, 172–178. https://doi.org/10.1006/eesa.1997.1623.
Flick, K., Kaiser, P., 2012. Protein degradation and the stress response. Semin. Cell Dev. Biol. 23, 515–522. https://doi.org/10.1016/j.semcdb.2012.01.019.
Gadd, G.M., Rhee, Y.J., Stephenson, K., Wei, Z., 2012. Geomycology: metals, actinides and biominerals. Environ. Microbiol. Rep. 4, 270–296. https://doi.org/10.1111/j.1758-2229.2011.00283.x.
Gallego, A., Martin-González, A., Ortega, R., Gutiérrez, J.C., 2007. Flow cytometry assessment of cytotoxicity and reactive oxygen species generation by single and binary mixtures of cadmium, zinc, and copper on populations of the ciliated protozoan *Tetrahymena thermophila*. Chemosphere 68, 647–661. https://doi.org/10.1016/j.chemosphere.2007.02.031.
Geva, P., Kahta, R., Nakonechny, F., Aronov, S., Nisnevitch, M., 2016. Increased copper bioremediation ability of new transgenic and adapted Saccharomyces cerevisiae strains. Environ. Sci. Pollut. Res. Int. 23, 19613–19625. https://doi.org/10.1007/s11356-016-7157-4.
Gillet, S., Lawarée, E., Matroule, J.-Y., 2019. Functional diversity of bacterial strategies to cope with metal toxicity. Microbial Diversity in the Genomic Era. 23. Elsevier, Inc., pp. 409–426. https://doi.org/10.1016/B978-0-12-814849-5.00023-X.
Gomes-Ferreira, M.D., Castro, J.A., Santana-Silva, R.J., Micheli, F., 2019. HVA22 from citrus: a small gene family whose some members are involved in plant response to abiotic stress. Plant Physiol. Biochem. 142, 395–404. https://doi.org/10.1016/j.plaphy.2019.08.003.
Grisvard, J., Aubusson-Fleury, A., Baroin-Tourancheau, A., 2010. Multiple uses of Lys63-polyubiquitination in the ciliate *Sterkiella histriomuscorum*. Protist. 161, 479–488. https://doi.org/10.1016/j.protis.2010.01.004.
Gutiérrez, J.C., De Francisco, P., Amaro, F., Díaz, S., Martin-González, A., 2019. Structural and functional diversity of microbial metallothionein genes. In: Das, S., Dash, H.R. (Eds.), Microbial Diversity in the Genomic Era. 22. Academic Press. Elsevier, pp. 387–407. https://doi.org/10.1016/B978-0-12-814849-5.00022-8.
Hamilton, C.A., Good, A.G., Taylor, G.J., 2001. Induction of vacuolar ATPase and mitochondrial ATP synthase by aluminum in an aluminum-resistant cultivar of wheat. Plant Physiol. 125, 2068–2077. https://doi.org/10.1104/pp.125.4.2068.
Holmes, A.O.M., Kalli, A.C., Goldman, A., 2019. The function of membrane integral pyrophosphatases from whole organism to single molecule. Front. Mol. Biosci. 6, 1–11. https://doi.org/10.3389/fmolb.2019.00132.
Homma, Y., Hiragi, S., Fukuda, M., 2021. Rab family of small GTPases: an updated vie won their regulation and functions. The FEBS J. 288, 36–55. https://doi.org/10.1111/febs.15453.
Hong, Y., Zhao, J., Guo, L., Kim, S.-C., Deng, X., et al., 2016. Plant phospholipases D and C and their diverse functions in stress responses. Prog. Lipid Res. 62, 55–74. https://doi.org/10.1016/j.plipres.2016.01.002.
Hu, J., Jiao, D., Xu, Q., Ying, X., Chi, Q., Ye, Y., Li, X., Cheng, L., 2016. Identification of proteasome subunit beta type 2 associated with deltamethrin detoxification in Drosophila Kc cells by cDNA microarray analysis and bioassay analyses. Gene. 582, 85–93. https://doi.org/10.1016/j.gene.2016.01.054.
Huang, Y., Agrawal, A.F., 2016. Experimental evolution of gene expression and plasticity in alternative selective regimes. PLoS Genet. 12 (9), 1–23. https://doi.org/10.1371/journal.pgen.1006336.
Hubbard, C., Singleton, D., Rauch, M., Jayasinghe, S., Cafiso, D., et al., 2000. The secretory carrier membrane protein family: structure and membrane topology. Mol. Biol. Cell 11, 2933–2947. https://doi.org/10.1091/mbc.11.9.2933.
Igarashi, J., Kobayashi, K., Matsuoka, A., 2011. A hydrogen-bonding network formed by the B10-E7-E11 residues of a truncated hemoglobin from *Tetrahymena pyriformis* is critical for stability of bound oxygen and nitric detoxification. J. Biol. Inorg. Chem. 16, 599–609. https://doi.org/10.1007/s00775-011-0761-3.
Imai, H., Nakagawa, Y., 2003. Biological significance of phospholipid hydroperoxide glutathione peroxidase (PHGPx, GPx4) in mammalian cells. Free Radic. Biol. Med. 34, 145–169. https://doi.org/10.1016/s0891-5849(02)01197-8.
Jackson, B.P., Williams, P.L., Lanzirotti, A., Bertsch, P.M., 2005. Evidence for biogenic pyromorphite formation by the nematode *Caenorhabditis elegans*. Environ. Sci. Technol. 39, 5620–5625. https://doi.org/10.1021/es050154k.
Jaishankar, M., Tseten, T., Anbalagan, N., Matehew, B.B., Beeregowda, K.N., 2014. Toxicity, mechanism, and health rffects of some heavy metals. Interdiscip. Toxicol. 7, 60–72. https://doi.org/10.2478/intox-2014-0009.
Jarostawiecka, A., Piotrowska-Seget, Z., 2014. Lead resistance in micro-organisms. Microbiology. 160, 12–25. https://doi.org/10.1099/mic.0.070284-0.
Jiang, L., Liu, X., Yin, H., Liang, Y., Liu, H., et al., 2020. The utilization of biomineralization technique based on microbial induced phosphate precipitation in remediation of potentially toxic ions contaminated soil: a mini review. Ecotoxicol. Environ. Saf. 191, 110009. https://doi.org/10.1016/j.ecoenv.2019.110009 1–9.
Juganson, K., Mortimer, M., Ivask, A., Kasemets, K., Kahru, A., 2013. Extracellular conversion of silver ions into silver nanoparticles by protozoan *Tetrahymena thermophila*. Environ. Sci. Proces. Impact. 15, 244–250. https://doi.org/10.1039/C2em30731f.
Kang, H., Hwang, I., 2014. Vacuolar sorting receptor-mediated trafficking of soluble vacuolar proteins in plant cell. Plants. 3, 392–408. https://doi.org/10.3390/plants3030392.
Kaur, G., Singh, H.P., Batish, D.R., Mahajan, P., Kohli, R.K., Rishi, V., 2015. Exogenous nitric oxide (NO) interferes with lead (Pb)-induced toxicity by detoxifying reactive oxygen species in hydroponically grown wheat (*Triticum aestivum*) roots. PLoS One 10 (9), e0138713. https://doi.org/10.1371/journal.pone.0138713 1-18.
Keasling, J.D., Van Dien, S.J., Pramanik, J., 1998. Engineering polyphosphate metabolism in *Escherichia coli*: implications for bioremediation of inorganic contaminants. Biotechnol. Bioeng. 58, 231–239. https://doi.org/10.1002/(sici)10970290(19980420)58:2/3<231::aidbit16>3.0.co;2-f.
Khan, A., Khan, S., Khan, M.A., Qamar, Z., Waqas, M., 2015. The uptake and bioaccumulation of heavy metals by food plants, their effects on plants nutrients, and associated health risk: a review. Environ. Sci. Pollut. Res. 22, 13772–13799. https://doi.org/10.1007/s11356-015-4881-0.
Kirsch, T., 2012. Biomineralization - an active or passive process? Connect. Tissue Res. 53, 438–445. https://doi.org/10.3109/03008207.2012.730081.
Klumpp, S., Krieglstein, J., 2002. Serine/threonine protein phosphatases in apoptosis. Curr. Opin. Pharmacol. 2, 458–462. https://doi.org/10.1016/s1471-4892(02)00176-5.
Klumpp, S., Krieglstein, J., 2009. Reversible phosphorylation of histidine residues in proteins from vertebrates. Sci. Signal. 2 (61), pe13. https://doi.org/10.1126/scisignal.261pe13.
Kovalchuk, I., Titov, V., Hohn, B., Kovalchuk, O., 2005. Transcriptome profiling reveals similarities and differences in plant responses to cadmium and lead. Mutat. Res. 570, 149–161. https://doi.org/10.1016/j.mrfmmm.2004.10.004.
Kumar, A., Prasad, M.N., 2018. Plant-lead interactions: transport, toxicity, tolerance, and detoxification mechanisms. Ecotoxicol. Environ. Saf. 166, 401–418. https://doi.org/10.1016/j.ecoenv.2018.09.113.
Kuroda, K., Ueda, M., 2010. Engineering of microrganisms towards recovery of rare metal ions. Appl. Microbiol. Biotechnol. 87, 53–60. https://doi.org/10.1007/s00253-010-2581-8.
Lander, N., Cordeiro, C., Huang, G., Docampo, R., 2016. Polyphosphate and acidocalcisomes. Biochem. Soc. Trans. 44, 1–6. https://doi.org/10.1042/BST20150193.
Law, A.H.Y., Chow, C-M., Jiang, L. 2012. Secretory carrier membrane proteins. Protoplasma. 249, 269–283. doi: https://doi.org/10.1007/s00709-011-0295-0.
Lecker, S.H., Goldberg, A.L., Mitch, W.E., 2006. Protein degradation by ubiquitin-proteasome pathway in normal and disease states. J. Am. Soc. Nephrol. 17, 1807–1819. https://doi.org/10.1681/ASN.2006010083.
Lee, C., Goldberg, J., 2010. Structure of coatomer cage proteins and the relationship among COPI, COPII, and clathrin vesicle coats. Cell. 142, 123–132. https://doi.org/10.1016/j.cell.2010.05.030.
Lee, J.-W., Choi, H., Hwang, U.-K., Kang, J.-C., Kang, Y.J., Kim, K.I., Kim, J.-H., 2019. Toxic effects of lead exposure on bioaccumulation, oxidative stress, neurotoxicity, and immune responses in fish: a review. Environ. Toxicol. Pharmacol. 68, 101–108. https://doi.org/10.1016/j.etap.2019.03.010.
Liang, X., Csetenyi, L., Gadd, G.M., 2016. Lead bioprecipitation by yeasts utilizing organic phosphorous substrates. Geomicrobiol J. 33, 294–307. https://doi.org/10.1080/01490451.2015.1051639.
Lilienbaum, A. 2013. Relationship between the proteasomal system and autophagy. Int J Biochem Mol Biol 4, 1–26. ISSN:2152–4114.
Liu, J.-J., 2017. Regulation of dynein-dynactin-driven vesicular transport. Traffic. 18, 336–347. https://doi.org/10.1111/tra.12475.
Liu, W., Tang, X., Qi, X., Fu, X., Ghimire, S., et al., 2020. The ubiquitin conjugating enzyme: an important ubiquitin transfer platform in ubiquitin-proteasome system. Int. J. Mol. Sci. 21 (2894), 1–16. https://doi.org/10.3390/ijms21082894.
Lu, L., Song, H.-F., Wei, J.-L., Liu, X.-Q., Song, W.-H., Yan, B.-Y., Yang, G.-J., Li, A., Yang, W.-L., 2014. Ameliorating replicative senescence of human bone marrow stromal cells by PSMB5 overexpression. Biochem. Biophys. Res. Commun. 443, 1182–1188. https://doi.org/10.1016/j.bbrc.2013.12.113.
Malik, A., 2004. Metal bioremediation through growing cells. Chemosphere 30, 261–278. https://doi.org/10.1016/j.envint.2003.08.001.
Martin-González, A., Díaz, S., Borniquel, S., Gallego, A., Gutiérrez, J.C., 2006. Cytotoxicity and bioaccumulation of heavy metals by ciliated protozoa isolated from urban wastewater treatment plants. Res. Microbiol. 157, 108–118. https://doi.org/10.1016/j.resmic.2005.06.005.
McMahon, H.T., Mills, I.G., 2004. COP and clathrin-coated vesicle budding: different pathways, common approaches. Curr. Opin. Cell Biol. 16, 379–391. https://doi.org/10.1016/j.ceb.2004.06.009.
Meireles, D.A., Domingos, R.M., Gaiarsa, J.W., Ragnoni, E.G., Bannitz-Fernandes, R., et al., 2017. Functional and evolutionary characterization of Ohr proteins in eukaryotes reveals many active homologs among pathogenic fungi. Redox Biol. 12, 600–609. https://doi.org/10.1016/j.redox.2017.03.026.
Menor-Salvan, C., 2012. Biomineralización de piromorfita en tuberías de plomo. Revista SEM (Sociedad Española de Mineralogía) 16, 158–159.
Miretzky, P., Fernandez-Cirelli, A., 2008. Phosphates for Pb immobilization in soils: a review. Environ. Chem. Lett. 6, 121–133. https://doi.org/10.1007/s10311-007-0133-y.
Naik, M.M., Dubey, S.K., 2013. Lead resistant bacteria: lead resistance mechanisms, their applications in lead bioremediation and biomonitoring. Ecotoxicol. Environ. Saf. 98, 1–7. https://doi.org/10.1016/j.ecoenv.2013.09.039.

Nakatsu, F., Hase, K., Ohno, H., 2014. The role of the clathrin adaptor AP-1: polarized sorting and beyond. Membranes. 4, 747–763. https://doi.org/10.3390/membranes4040747.
Nandi, D., Tahiliani, P., Kumar, A., Chandu, D., 2006. The ubiquitin-proteasome system. J. Biosci. 31, 137–155. https://doi.org/10.1007/BF02705243.
Nilsson, J.R., 1989. *Tetrahymena* in Cytotoxicology: with special reference to effects of heavy metals and selected drugs. Eur. J. Protistol. 25, 2–25. https://doi.org/10.1016/S0932-4739(89)80074-4.
Okorokov, L.A., Lichko, L.P., Kulaev, I.S., 1980. Vacuoles: main compartments of potassium, magnesium, and phosphate ions in *Saccharomyces carlsbergenis* cells. J. Bacteriol. 144, 661–665. https://doi.org/10.1128/jb.144.2.661-665.1980.
Pérez-Castiñeira, J.R., Gómez-García, R., López-Marqués, R.L., Losada, M., Serrano, A., 2001. Enzymatic systems of inorganic pyrophosphate bioenergetics in photosynthetic and heterotrophic protists: remnants or metabolic cornerstones? Int. Microbiol. 4, 135–142. https://doi.org/10.1007/s10123-001-0028-x.
Pérez-Castiñeira, J.R., Alvar, J., Ruíz-Pérez, L.M., Serrano, A., 2002. Evidence for a wide occurrence of proton-translocating pyrophosphatase genes in parasitic and free-living protozoa. Biochem. Biophys. Res. Commun. 294, 567–573. https://doi.org/10.1016/S0006-291X(02)00517-X.
Piersanti, A., Juganson, K., Mozzicafreddo, M., Wei, W., Zhao, K., Ballarini, P., Mortimer, M., Pucciarelli, S., Miao, W., Miceli, C., 2021. Transcriptomic responses to silver nanoparticles in the freshwater unicellular eukaryote *Tetrahymena thermophila*. Environ. Pollut. 269, 115965. https://doi.org/10.1016/j.envpol.2020.115965.
Rahaman, A., Miao, W., Turkewitz, A.P., 2009. Independent transport and sorting of functionally distinct protein families in *Tetrahymena thermophila* dense core secretory granules. Eukaryot. Cell 8, 1575–1583. https://doi.org/10.1128/EC.00151-09.
Rahman, Z., Singh, V.P., 2020. Bioremediation of toxic heavy metals (THMs) contaminated sites: concepts, applications, and challenges. Environ. Sci. Pollut. Res. Int. 27, 27563–27581. https://doi.org/10.1007/s11356-020-08903-0.
Rawlings, N.D., Tolle, D.P., Barrett, A.J., 2004. MEROPS: the peptidase database. Nucl. Acids Res. 32, D160–D164. https://doi.org/10.1093/nar/gkh071.
Rhee, Y.J., Hillier, S., Gadd, G.M., 2012. Lead transformation to pyromorphite by fungi. Curr. Biol. 22, 237–241. https://doi.org/10.1016/j.cub.2011.12.017.
Rhee, Y.J., Hillier, S., Pendiowski, H., Gadd, G.M., 2014. Pyromorphite formation in a fungal biofilm community growing on lead metal. Environ. Microbiol. 16, 1441–1451. https://doi.org/10.1111/1462-2920.12416.
Rigden, D.J., 2008. The histidine phosphatase superfamily: structure and function. Biochem. J.409, 333–348. https://doi.org/10.1042/BJ20071097.
Sarkar, S., Mukberjee, A., Parvin, R., Das, S., Roy, U., et al., 2019. Removal of Pb(II), As(III), and Cr(VI) by nitrogen-starved *Papiliotrema laurentii* strain RY1. J. Basic Microbiol. 1–15 https://doi.org/10.1002/jobm.201900222.
Sauer, U., 2001. Evolutionary engineering of industrially important microbial phenotypes. Adv. Biochem. Eng. Biotechnol. 73, 129–169. https://doi.org/10.1007/3-540-45300-8_7.
Scheckel, K.G., Diamond, G.L., Burgess, M.F., Klotzbach, J.M., Maddaloni, M., et al., 2013. Amending soils with phosphate as means to mitigate soil lead hazard: a critical review of the state of the science. J. Toxicol. Environ. Health B 16, 337–380. https://doi.org/10.1080/10937404.2013.825216.
Schöneberg, J., Lee, I.-H., Iwasa, J.H., Hurley, J.H., 2016. Reverse-topology membrane scission by the ESCRT proteins. Nat. Rev. Mol. Cell Biol. 18, 5–17. https://doi.org/10.1038/nrm.2016.121.
Sekiya, F., 2013. Phospholipase. In: Lennarz, W.J., Lane, M.D. (Eds.), Encyclopedia Biol. Chem., Second edition Academic Press, pp. 467–471
Sharma, P., Dubey, R.S., 2005. Lead toxicity in plants. Braz. J. Plant Physiol. 17, 35–52. https://doi.org/10.1590/S1677-04202005000100004.
Shen, H., Sikorska, M., LeBlanc, J., Walker, P.R., Liu, Q.Y., 2006. Oxidative stress regulated expression of ubiquitin carboxyl-terminal hydrolase-L1: role in cell survival. Apoptosis. 11, 1049–1059. https://doi.org/10.1007/s10495-006-6303-8.
Silbergeld, E.K., Waalkes, M., Rice, J.M., 2000. Lead as a carcinogen: experimental evidence and mechanisms of action. Am. J. Ind. Med. 38, 316–323. https://doi.org/10.1002/1097-0274(200009)38:3<316::aid-ajim11>3.0.co;2-p.
Singh, K., Bhori, M., Kasu, Y.A., Bhat, G., Marar, T., 2018. Antioxidants as precision weapons in war against cancer chemotherapy induced toxicity. Exploring the armory of obscurity. Saudi Pharm. J. 26, 177–190. https://doi.org/10.1016/j.jsps.2017.12.013.
Syutkin, A.S., Pyatibratov, M.G., Galzitskaya, O.V., Rodriguez-Valera, F., Federov, O.V., 2014. *Haloarcula marismortui* archaellin genes as ecoparalogs. Extremophiles. 18, 341–349. https://doi.org/10.1007/s00792-013-0619-4.
Tansey, W.P., 1999. How cells use proteolysis to control their growth. Mol. Med. 5, 773–782. https://doi.org/10.1007/BF03401990.
Tchounwou, P.B., Yedjou, C.G., Patlolla, A.K., Sutton, D.J., 2012. Heavy metals toxicity and the environment. Mol. Clin. Environ. Toxicol. 101, 133–164. https://doi.org/10.1007/978-3-7643-8340-4_6.
Templeton, A.S., Trainor, T.P., Spormann, A.M., Newville, M., Sutton, S.R., et al., 2003. Sorption versus biomineralization of Pb(II) within *Burkholderia cepacia* biofilms. Environ. Sci. Technol. 37, 300–307. https://doi.org/10.1021/es025972g.
Tuvim, M.J., Adachi, R., Hoffenberg, S., Dickey, B.F., 2001. Traffic control: Rab GTPases and the regulation of interorganellar transport. News Physiol. Sci. 16, 56–61. https://doi.org/10.1152/physiologyonline.2001.16.2.56.
Verma, R., Aravind, L., Oania, R., McDonald, W.H., Yates, J.R., Koonin, E.V., Deshaies, R.J., 2002. Role of Rpn11 metalloprotease in deubiquitination and degradation by the 26S proteasome. Science. 289, 611–615. https://doi.org/10.1126/science.1075898.
Virgolini, M.B., Aschner, M., 2021. Molecular mechanisms of lead neurotoxicity (chapter five). In: Aschner, M., Costa, L.G. (Eds.), Advances in Neurotoxicology. 5. Academic Press-Elsevier, pp. 159–213. https://doi.org/10.1016/bs.ant.2020.11.002.
Waalkes, M.P., Harvey, M.J., Klaassen, C.D., 1984. Relative in vitro affinity of hepatic metallothionein for metals. Toxicol. Lett. 20, 33–39. https://doi.org/10.1016/0378-4274(84)90179-6.
Wang, J., Chen, C., 2006. Biosorption of heavy netals by *Saccharomyces cerevisiae*: a review. Biotechnol. Adv. 24, 427–451. https://doi.org/10.1016/j.biotechadv.2006.03.001.
Wang, X., Wang, H., 2020. Priming the proteasome to protect against proteotoxicity. Trends Mol. Med. 26, 639–646. https://doi.org/10.1016/j.molmed.2020.02.007.
Wannhoff, A., Bolck, B., Kubler, A.C., Bloch, W., Reuther, T., 2013. Oxidative and nitrosative stress and apoptosis in oral mucosa cells after *ex vivo* exposure to lead and benzo[a]pyrene. Toxicol. In Vitro 27, 915–921. https://doi.org/10.1016/j.tiv.2013.01.007.
Wera, S., Hemmlngst, B.A., 1995. Serine/threonine protein phosphatases. Biochem. J. 311, 17–29. https://doi.org/10.1042/bj3110017.
Williams, D.L., Bonilla, M., Gladyshev, V.N., Salinas, G., 2013. Thioredoxin glutathione reductase-dependent redox networks in platyhelminth parasites. Antioxid. Redox Signal. 19, 735–745. https://doi.org/10.1089/ars.2012.4670.
Wu, W., Huang, H., Ling, Z., Yu, Z., Jiang, Y., et al., 2016b. Genome sequencing reveals mechanisms for heavy metal resistance and polycyclic aromatic hydrocarbon degradation in *Delftia lacustris* strain LZ-C. Ecotoxicology 25, 234–247. https://doi.org/10.1007/s10646-015-1583-9.
Wu, X., Cobbina, S.J., Mao, G., Xu, H., Zhang, Z., 2016a. A review of toxicity and mechanisms of individual and mixtures of heavy metals in the environment. Environ. Sci. Pollut. Res. 23, 8244–8259. https://doi.org/10.1007/s11356-016-6333-x.
Yap, C.K., Tan, W.S., Wong, K.W., Ong, G.H., Cheng, W.H., et al., 2021. Antioxidant enzyme activities as biomarkers of Cu and Pb stress in *Centella asiatica*. Stresses. 1, 253–265. https://doi.org/10.3390/stresses1040018.
Yedidi, R.S., Wendler, P., Enenkel, C., 2017. AAA-ATPases in protein degradation. Front. Mol. Biosci. 4 (42), 1–14. https://doi.org/10.3389/fmolb.2017.00042.
Zamzami, M.A., 2022. Inosine triphosphate pyrophosphatase (ITPase): functions, mutations, polymorphisms, and its impact on cancer therapies. Cells. 384, 1–11. https://doi.org/10.3390/cells11030384.
Zhang, F., Hu, Y., Huang, P., Toleman, C.A., Paterson, A.J., et al., 2007. Proteasome function is regulated by cyclic AMP-dependent protein kinase through phosphorylation of Rpt6. J. Biol. Chem. 282, 22460–22471. https://doi.org/10.1074/jbc.M702439200.
Zhao, X., Petursson, F., Viollet, B., Lotz, M., Terkeltaub, R., et al., 2014. Peroxisome proliferator-activated receptor γ coactivator 1α and FoxO3A mediate chondroprotection by AMP-activated protein kinase. Arthritis Rheum. 66, 3073–3082. https://doi.org/10.1002/art.38791.